Master's Thesis

Charge-Modulated Synthesis of Highly Stable

Iron Oxide Nanoparticles for Bio-Application

Sunyoung Woo

Department of Chemical Engineering

Graduate School of UNIST

2019

Charge-Modulated Synthesis of Highly Stable Iron Oxide Nanoparticles for Bio-Application

Sunyoung Woo

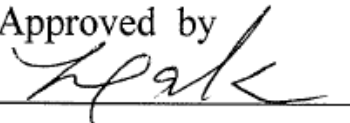Department of Chemical Engineering

Graduate School of UNIST

Charge-Modulated Synthesis of Highly Stable Iron Oxide Nanoparticles for Bio-Application

A thesis/dissertation

submitted to the Graduate School of UNIST

in partial fulfillment of the

requirements for the degree of

Master of Science

Sunyoung Woo

06/10/2019 of submission

Approved by
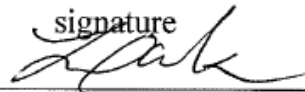
_____

Advisor

Jongnam Park

Charge-Modulated Synthesis of Highly Stable Iron Oxide Nanoparticles for Bio-Application

Sunyoung Woo

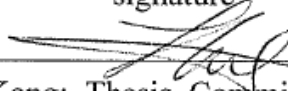This certifies that the thesis/dissertation of Sunyoung Woo is approved.
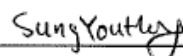
06/10/2019 of submission

signature

_____
Advisor: Jongnam Park

signature

_____
Sebyung Kang: Thesis Committee Member #1

signature

_____
Sung You Hong: Thesis Committee Member #2

Abstract

Iron oxide nanoparticles (IONPs) have received considerable attention owing to its various biomedical application, including magnetic resonance imaging contrast agent, cancer targeting, and drug delivery. For the in-vivo application, the IONPs are required to be highly stable and biocompatible. However, the IONPs initially synthesized in organic solvent have hydrophobic ligands and they are unstable and toxic in physiological conditions. Therefore, surface modification of the IONPs must be considered to change hydrophobic ligands into hydrophilic ligands for bio-application. After the surface modification, physical properties of the IONPs are modified such as size, shape, hydrophobicity, surface charge, and coating materials. Especially, the surface charge of the IONPs is one of the most important factors because it affects colloidal stability of the IONPs and interactions with biomolecule in physiological condition. In our study, we fabricated highly stable and non-toxic IONPs via surface modification and tested their biocompatibility and potential for bio-functionalization. To process the surface modification, we synthesized PEG-based three different charged ligands via reversible addition-fragmentation chain transfer-mediated (RAFT) polymerization and conducted the toxicological evaluation *in vitro* and *in vivo*. All of the charged IONPs showed long-term colloidal stability during three months in aqueous solution without agglomeration and no significant cellular damage in the A549, Huh-7, and SH-SY5Y cells. The charged IONPs have no significant toxicity in balb/c mice. We further developed more stable multidentate catechol-based zwitterionic ligand (MCZ-ligand) compared to polyethylene glycol-based ligands via RAFT polymerization. The IONPs coated with MCZ-ligand showed superior colloidal stability in a wide ranges of pH and saline solution for 1 year and low nonspecific adsorption with bovine serum albumin proteins. Furthermore, we confirmed the potential for bio-functionalization of the MCZ-IONPs. Biomolecules, biotin and streptavidin were conjugated on the MCZ-IONPs via carbodiimide chemistry and the bio-functionalization was confirmed via strong interaction between biotin and streptavidin. Consequently, our charged IONPs and zwitterionic IONPs performed excellent colloidal stability and non-toxicity in physiological conditions. These results open a possibility for biomedical application of the IONPs.

Contents

List of Figures

List of Abbreviation

IONPs	iron oxide nanoparticles
MRI	magnetic resonance imaging
OAc-IONPs	oleic acid-coated IONPs
PEG	polyethylene glycol
H.D	hydrodynamic diameter
RAFT	reversible addition-fragmentation chain transfer-mediated
negative ligand	(-) ligand
neutral ligand	(n) ligand
positive ligand	(+) ligand
PDI	polydispersity index
negatively charged IONPs	(-) IONPs
neutral IONPs	(n) IONPs
positively charged IONPs	(+) IONPs
DIW	deionized water
DMA	N-[2-(3,4-Dihydroxyphenyl)ethyl]-2-methylprop-2-enamide
DMEM	Dulbecco's modified Eagle's medium
TEM	transmission electron microscopy
NMR	nuclear magnetic resonance
GPC	gel permeation chromatography
DLS	dynamic laser scattering
BUN	blood urea nitrogen
CREA	creatinine
ALT	alanine aminotransaminase
ALP	alkaline phosphatase
AST	aminotransaminase
TBIL	total bilirubin

DP	degree of polymerization
MCZ-ligand	multidentate catechol-based zwitterionic ligand
MCZ-IONPs	MCZ-ligand coated IONPs
ZMA	3-(Methacryloylamino)propyl]dimethyl(3-sulfopropyl)ammonium hydroxide inner salt
EDC	N-(3-Dimethylaminopropyl)-N′-ethylcarbodiimide hydrochloride

I. Introduction

1.1 Iron Oxide Nanoparticles and Basic Properties

Nanomaterials are defined as materials with one, two, or three external dimensions ranging from 1 to 100 nm-the nanoscale.[1] The uniform nanomaterials show many attractive properties such as electrical, optical, magnetic, and chemical properties, which cannot be accomplished by their bulk counterparts.[2] Among nanomaterials, magnetic nanoparticles (MNPs) with unique superparamagnetism, biocompatibility, and good stability have been extensively studied in many biomedical fields such as drug delivery, hyperthermia, magnetic resonance imaging (MRI), catalysis, data storage, electronic communication, and environmental remediation etc.[3] Superparamagnetic iron oxide nanoparticles (SPIONs) consist of iron oxide cores such as magnetite (Fe_3O_4), maghemite (γ-Fe_2O_3) and hematite (α-Fe_2O_3). Both maghemite and magnetite are traditionally ferromagnetic in nature with saturation magnetization reaching to 92 emu g^{-1}. However, they lose their permanent magnetism and become superparamagnetic when they are decreased in size to 30 nm or smaller.[1] Iron oxide nanoparticles (IONPs) also have various unique properties such as high surface-to-volume ratio or size dependent magnetic properties, low toxicity and easy modification. With these properties, the IONPs can be applied for bio-medical fields.

There are many methods to synthesize IONPs such as co-precipitation method, hydrothermal reactions, thermal decomposition, microemulsion method, sol-gel reactions, aerosol/vapor phase method, and electrochemical method etc.[4] Among them, thermal decomposition method has unique advantages of good control of size and shapes, and high yield. However, synthesized IONPs has hydrophobic ligands like oleic acid during the thermal decomposition process. Therefore, surface modification of the oleic acid-coated IONPs (OAc-IONPs) with a hydrophilic ligand must be required for bio-application (**Figure 1**).
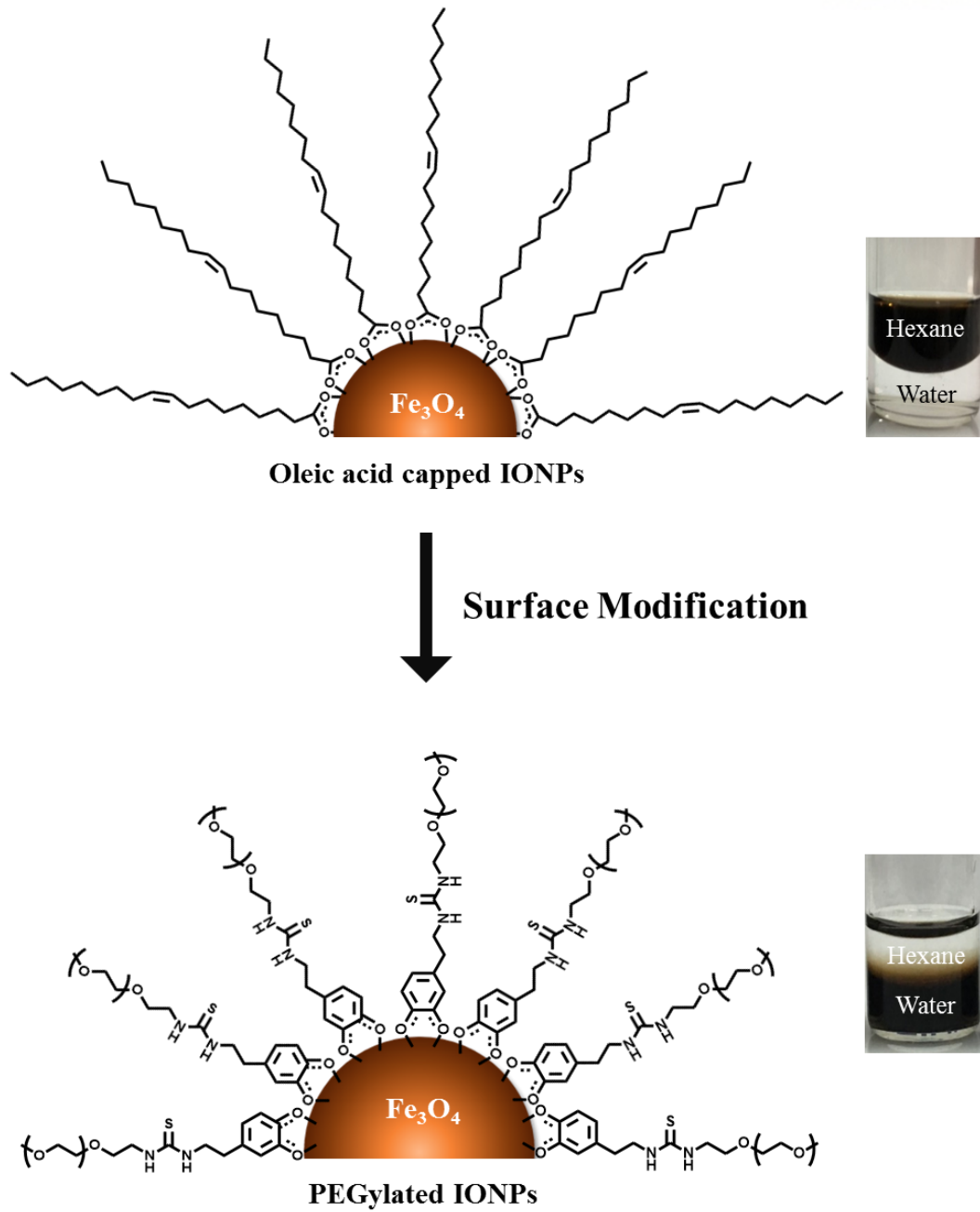
Figure 1. Surface modification of OAc-IONPs.

1.2 Surface Modification of IONPs

Surface medication of IONP is a crucial process because of following reasons: (1) Maintenance of the unique properties; (2) Enhancement of colloidal stability of IONPs without aggregation; (3) Improvement of the surface activity of IONPs for functionalization with useful molecule; (4) Biocompatibility, non-toxicity in biological condition, and stealth function from immune system; (5) Long-term circulation in physiological conditions. Through the surface modification, IONPs can be facilitated for biomedical application.

For the surface modification of IONPs, there are three main methods; encapsulation and ligand exchange. First, encapsulation needs amphiphilic polymer which has both hydrophobic parts and hydrophilic parts. IONPs capped with hydrophobic ligands are coated with the amphiphilic polymers again. The inserted hydrophobic parts of amphiphilic polymers can interact with the hydrophobic ligands on IONPs. The hydrophilic parts of amphiphilic polymers render the IONPs water-dispersible in aqueous solution. The functional group of amphiphilic polymers also allows IONPs to be bio-conjugated.[5] Second, ligand exchange is one of the main methods for simply making IONPs soluble in aqueous solution by substituting the hydrophobic ligands with hydrophilic materials.[6-7] The ligands are composed of anchoring group, hydrophilic group, and functional group. Anchoring group should have strong affinity to surface of IONPs because the ligands competitively substitute the hydrophobic ligands. An incomplete exchange or irreversible adsorption of the ligand can cause low colloidal stability in aqueous solution or biological conditions. To solve this problem, bidentate or multidentate anchoring groups can be introduced because they have high binding affinity onto IONPs. Compared to monomeric ligands, multidentate ligands can improve the colloidal stability.

There are biocompatible inorganic or organic materials used for surface modification of IONPs. The functionalized IONPs have been utilized in various bio-application fields such as biolabeling, bioseparation, and catalysis.[5] First, a variety of inorganic materials have been studied including silica, metal, metal oxides, sulfides, and nonmetals to provide IONPs biocompatibility. Silica-coated IONPs were colloidally stable, photostable, and water-stable.[8] Gold shells enabled easy modification by thiol-containing ligands and its gold-coated IONPs were quite stable because of their inertness. Second, organic compounds offering functional groups such as carboxylate, amine, hydroxyl, and aldehyde groups are easily able to bio-functionalize IONPs. Biomolecules such as DNA, protein, antibody, enzyme, and other nano-biomolecules can be linked to IONPs by introducing the organic functional groups, In addition, organic materials can provide IONPs biocompatibility from monomer to macro molecules such as citrate, phosphate, liposomes, proteins, and polymers. Many polymers have been

studied for biocompatible IONPs. For example, there are natural polymers like dextran and chitosan, and synthetic polymer like polyethylene glycol(PEG), polyethylenimine, polyacrylic acids and so on. When introducing organic compounds, we have to consider following subjects of IONPs such as controlling of shape, surface structure, stability, biocompatibility, and magnetic properties of IONPs.

1.3 Bio-Application and Toxicity Studies of IONPs

Bio-functionalization of IONPs is one of the most important topics for the bio-application. There are two main strategies for bio-functionalization; one is non-covalent strategies and the other is covalent strategies. Non-covalent strategies use physical interactions between IONPs and bio-molecules for instance ionic coupling, hydrophobic coupling, biotin-avidin system and so on. Although these non-covalent strategies have an advantage of easy functionalization, the conjugation is unstable and reproducibility is very low. On the contrary, the covalent coupling can make the IONPs obtain more stable and stronger conjugation with bio-molecules such as antibodies, enzymes, oligonucleotides, carbohydrates, peptides, or surface receptors by introducing amine, aldehydes, and epoxides groups. There are representative covalent coupling strategies including EDC coupling reaction, maleimide coupling, and click-chemistry reaction.[9] Among them, EDC coupling reaction is the most widely introduced method because of its advantages. For the EDC coupling, carbodiimide is used to activate the reaction between carboxylate and amine for forming amide bond, which can be applicable to numerous molecules. EDC coupling can be conducted in various organic or hydrophilic solution and it also can easily eliminate by-product via dialysis or gel-filtration after the reaction. Maleimide coupling generally uses thiol reactive maleimide group for a conjugation with primary amine and thiols and the reaction is often introduced in the gold nanoparticles because of the strong affinity between thiol and gold nanoparticles.[10] Click-chemistry reaction is easy, fast, and bio-orthogonal reaction, which can be effectively applied both in vitro and in vivo with specific interaction. Cupper (I)-catalyzed azide-alkyne cycloaddition (CuAAC) is one of the classic methods in the Click-chemistry reaction by using cupper catalyst for forming 5-membered heteroatom ring from azide and alkyne where cupper can cause cytotoxicity. To lower the toxicity, strain-promoted azide-alkyne cycloaddition (SPAAC) was developed without cupper by introducing a strained difluorooctyne and the SPAAC successfully utilized to prove for azide in living systems.[11-12] Through these bio-functionalization, the IONPs can be applied in various biomedical fields e.g., diagnostic, cancer targeting, drug delivery, imaging, MRI contrast agent, magnetic hyperthermia, immunoassay, tissue repair, and cell tracking.

However, prior to application of IONPs in the bio-medical fields, the toxicity studies on surface modified IONPs must be conducted because surface modification directly have an influence on cell/tissue biodistribution and clearance/metabolization.[13] Generally plain IONPs pose a low health hazard because Fe is a naturally occurring metal in the human body. As the body is adapted to metabolizing the particles into its elements, IONPs can be utilized in the body via subsequent metabolic processes.[14] However, surface functionalized IONPs can result in very different cellular responses as mentioned above. There are various factors influencing the cytotoxicity, e.g., size, shape, surface charge,

hydrophobicity, surface porosity, and roughness. In cells, NP-cell interaction can influence cellular uptake and internalization, and further affect cell morphology, proliferation, cytoskeleton, differentiation, and survival.[13] *In vivo*, IONPs injected via intravenously injection can be almost cleared from the systemic circulation by macrophages residing in the reticuloendothelial.[15] After being taken up into the cells via receptor-mediated endocytosis, the IONPs can be metabolized in the lysosomal compartments[16] and free iron can be circulated in the body naturally. Therefore, the small quantities of injected IONPs do not cause toxicity issues although high amounts can lead to a toxicity in body. **Figure 2** shows drainage route of nanoparticles through different organs according to their size property.
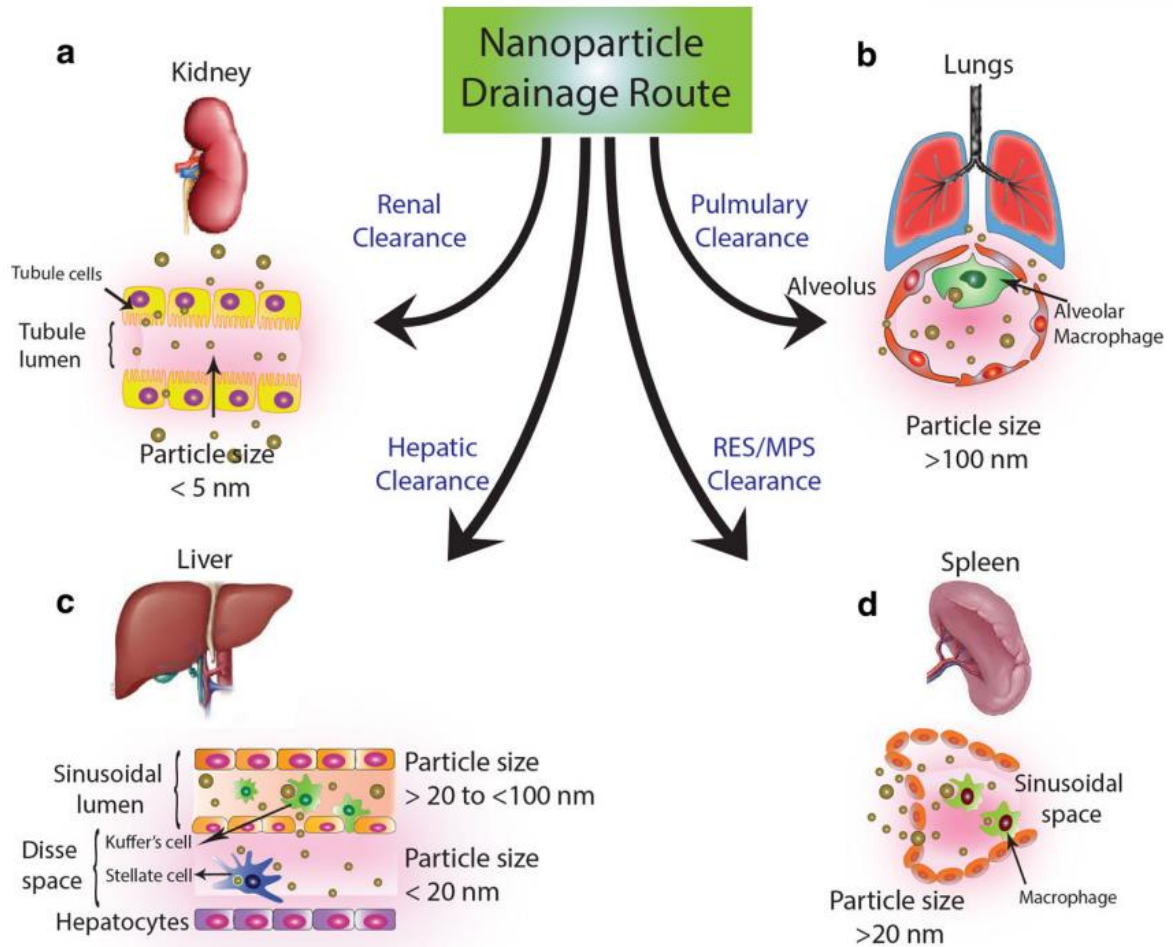
Figure 2. Drainage route of nanoparticles through different organs.[17]

II. Synthesis of Different Charged Iron Oxide Nanoparticles via RAFT Polymerization for *In Vitro* and *In Vivo* Toxicity Evaluation

2.1. Introduction

IONPs have promising potential in various biomedical fields such as MRI contrast agents, biosensors, hyperthermia, drug delivery, cancer targeting, transfection, cell tracking, and tissue repair because of their low toxicity, magnetic properties, and easy surface-modification.[18-23] In order to apply the IONPs to the bio-application, the IONPs should have excellent colloidal stability, ability of functionalization with biomolecules, and non-toxicity in physiological condition.[24]

Through the surface modification process, the IONPs can be stable and biocompatible in the biological environment and have a useful functional groups capable of binding to various biomolecules.[25-27] However, in the surface modification process, surface physi-co-chemical properties of IONPs could be changed inevitably during the surface modification process such as hydrodynamic diameter (H.D), shape, porosity, and surface charge of IONPs. Among these properties, it is well known that the change of the surface charge significantly influences cytotoxicity because it directly has an effect on the interaction between the charged IONPs and biological components.[28]

Many research groups have studied the effect of the charged IONPs based on cytotoxicity, genotoxicity, and neurotoxicity.[29-33] However, there has been a limitation of colloidal stability and chemical structure of surface ligand on the charged IONPs. For example, the charged IONPs can induce nonspecific interaction with proteins, and the phenomenon promotes another interaction between the charged IONPs and cells. This protein corona increasing H.D of particles induces the precipitation of nanoparticles and consequently causes the toxicity from particle uptake, pharmacokinetics, and bio-distribution.[34-35] Furthermore, almost studies on the charged IONPs involve variable in toxicity evaluation because of the different chemical structures of the ligand. Rivet et al.[36] demonstrated that the charged IONPs were synthesized by using aminosilane, dextran, and poly-(dimethylamine-co-epichlorhydrin-co-ethylendiamine for the cortical neuron cytotoxicity and showed a correlation between metabolic activity and surface charge. However, the other properties except for surface charge decorated with varieties of amine, alcohol, and zwitterion ligands, can also have another unpredictable effect on cytotoxicity. Therefore, for an accurate evaluation of cytotoxicity based on the surface charge by itself, the material must have high colloidal stability in a biological condition and minimize other variables in structure.

In this dissertation, we designed three different charged IONPs for enhancing the colloidal stability and minimizing the other variable in structure by using reversible addition-fragmentation chain transfer-mediated (RAFT) polymerization method to systematically evaluate the *in vitro* and *in vivo* toxicity. The RAFT polymerization method has the advantage of controlling the ratio of the constituent materials, the molecular weight of the polymer, and polydispersity to exhibit uniform surface characteristics as desired.[37] We synthesized three different charged polymeric ligands via RAFT polymerization; negative ligand ((-) ligand) used carboxyl group, neutral ligand ((n) ligand) based PEG moiety, and positive ligand ((+) ligand) used amine group. They had the same backbone and low polydispersity index (PDI) values. Subsequently, we made the three different charged IONPs (negatively charged IONPs ((-) IONPs), neutral IONPs ((n) IONPs), and positively charged IONPs ((+) IONPs)) by ligand exchange to evenly coat the surface of IONPs. The colloidal stability of the charged IONPs lasted for three months in deionized water (DIW) without changing their initial characteristics. We further evaluated the cytotoxicity of three IONPs in three different human cell lines; human lung cancer cell, human liver cancer cell, and human neural cancer cell by investigating viability change (MTT assay) and morphological alteration on the cells (confocal microscopy). In addition, *in vivo* toxicity study was performed by hematological analysis and histological analysis in mice. Notably all of our synthesized IONPs with superior colloidal stability showed excellent biocompatibility *in vivo* and *in vitro* test.

2.2 Materials and Experimental Section

2.2.1 Materials. Iron(III) chloride hexahydrate, oleic acid, Dimethyl sulfoxide, Polyethylene glycol methyl ether acrylate (average Mn 480), acrylic acid, and Thiazolyl blue tetrazolium bromide were purchased from Sigma Aldrich (Korea). Sodium oleate, N-[3-Dimethylamino)propyl]acrylamide, and 2-(2-Aminoethoxy)ethanol were purchased from TCI. 2,2'-Azobisisobutyronitrile was purchased from Samchun. N-[2-(3,4-Dihydroxyphenyl)ethyl]-2-methylprop-2-enamide (DMA), and dibenzyl trithiocarbonate were synthesized as previous reported method.[38-39] A549, Huh-7, and SH-SY5Y were purchased from ATCC. RPMI 1640, Dulbecco's modified Eagle's medium (DMEM), Penicillin-Streptomycin, and Trypsin/EDTA were purchased from Lonza. Fetal bovine serum was purchased from Gibco. DPBS was purchased from Welgene.

2.2.2 Synthesis of OAc-IONPs. OAc-IONPs which have high crystallinity and uniform size distribution were synthesized by previously described thermal decomposition method.[40] Briefly, 1 mmol of iron oleate complex and 0.73 mmol of oleic acid were dissolved in 1.5 g 1-octadecene. The mixture was heated up to 320°C for 1 h 30 min, and kept at the temperature for 30 min. The nanoparticles were cooled to room temperature, and precipitated using 50 mL acetone and ethanol mixed solvent by centrifugation to obtain purified nanoparticles. The size and morphologies of nanoparticles were observed by transmission electron microscopy (TEM).

2.2.3 Synthesis of Different Charged Polymer Ligands. We synthesized different charged polymeric ligands by RAFT polymerization method using different functional group to provide different charge on IONPs.[37] For synthesis of the (n) ligand, (-) ligand, and (+) ligand, we used PEG, acrylic acid and tertiary amine as functional group respectively. All of the polymers were equally composed of 20% of DMA and 60% of PEG groups, 20% of functional groups. All monomers (1 mmol) were mixed in 1 mL N,N-Dimethylformamide and dibenzyl trithiocarbonate (RAFT reagent, 50 μmol) and 2,2'-Azobisisobutyronitrile were added in 5 mL ampule. Freeze-pump-thaw cycles were repeated 4 times, and the ampule was sealed under vacuo using a torch gas. The ampule was heated up to 70°C for overnight and after reaction, the excess residues were washed with ethyl ether by centrifugation with three times. Solvent was removed in vacuum oven to obtain the polymer products.

2.2.4 Synthesis of Different Charged IONPs. Ligand exchange method were used to modify OAc-IONPs with synthesized polymer ligands. We mixed OAc-IONPs (5 mg), each polymer (30 mg) and 2-(2-Aminoethoxy)ethanol (100 mg) in $CHCl_3$, and react for 12 h at 60°C. After reaction, the solution was precipitated using diethyl ether by centrifugation (3 min, 3000 rpm) and dissolved in DIW. To remove the excess reagent, we used a centrifugal filter (MWCO 50 k) and washed out three times.

2.2.5 Characterization. TEM images were observed on JEM-2100F (JEOL) which was operated at 200 kV. Polymers were analyzed by ^{1}H nuclear magnetic resonance (NMR) using AVANCE III HD (Bruker) instrument at 400 MHz using deuterated chloroform solution. Molecular weight and molecular weight distribution were analyzed by gel permeation chromatography (GPC) (Shimadzu, RI detector). H.D, size distribution, and zeta-potentials of the IONPs in DIW and cell culture media were determined by dynamic laser scattering (DLS) particles size analyzer Nano-ZS90 (Malvern). All measurements were performed in 400 μL disposable cuvette using a 4 mW He-Ne laser operating at a wavelength of 633 nm at 25°C and the scattering angle was fixed at 90°. Zeta-potentials were measured to confirm surface charge of the IONPs. Samples were prepared in DIW or cell culture media by diluting.

2.2.6 Cell Lines and Cell Culture. The used cell lines are A549, Huh-7, and SH-SY5Y. Each cell was cultured in different suitable media and A549 and Huh-7 were cultured in RPMI 1640, SH-SY5Y in DMEM supplemented with 10% fetal bovine serum, 100 IU/mL penicillin, and 100 μg/mL streptomycin at 37°C under 5% CO_2 in humidified incubator.

2.2.7 MTT Assay. Cell viability was measured using MTT assay. For the test, the cells were seeded into 96-well flat-bottom plates at a starting density of 1 x 10^4 cells per well (A549 and Huh-7), and 4 x 10^4 (SH-SY5Y) cells per well. All cells were cultured for 24 h, the IONPs were treated in each well and incubated for 24 h. After that IONPs were washed by DPBS three times and 10 μL (5 mg/mL) of thiazolyl blue tetrazolium bromide solution was added to each of 96 wells for 3 h at 37°C CO_2 incubator. Cells were lysed with 150 μL of dimethyl sulfoxide and absorbance was measured by microplate reader (GloMax® Discover, Promega) at 560 nm wavelength.

2.2.8 Animal. Balb/c mice (male, 6 weeks) were purchased from the Orient-Bio Co. (Seongnam, Korea) and the mice were adapted for 7 day under environmentally controlled animal room conditions of a temperature (23±3°C), relative humidity (50±20%), and air ventilation of 10–20 times/h with a 12/12 h light/dark cycle.

2.2.9 Hematological and Histological Analysis. The mice were randomly grouped and the IONPs were treated by intravenous injection of 2 mg Fe/kg (low dose, $n = 3$) and 10 mg Fe/kg (high dose, $n = 3$) for 24 h once to observe acute toxicity. 1X PBS was used as negative control. Blood was collected from the caudal vena cava and serum was obtained by centrifugation at 3,000 rpm for 10 min at room temperature. Blood urea nitrogen (BUN), creatinine (CREA), alanine aminotransaminase (ALT), alkaline phosphatase (ALP), aspartate aminotransaminase (AST), total bilirubin (TBIL) were measured using a Dry Chem-3000 autoanalyzer (FujiFilm, Tokyo, Japan). Histological toxicity was rated from level 0 to level 5 in six organ; liver, kidney, lung, heart, spleen, and brain.

2.3 Results and Discussion

2.3.1 Synthesis and Characterization of OAc-IONPs and Different Charged Ligands. For the clinical application of IONPs such as MRI contrast agents, it is important to synthesize homogeneous IONPs because magnetic properties and surface properties depend on the size of the IONPs,[27] so we synthesized monodisperse OAc-IONPs by using a thermal decomposition method which can effectively control the size, polydispersity, and shape of the NPs with large quantities.[40] As shown in **Figure 3a**, the uniform distribution of OAc-IONPs was observed (about 11.6 ± 0.7 nm) by TEM. The H.D of OAc-IONPs was characterized by DLS measurement confirming that the size of Oac-IONP was about 14.58 nm and PDI value was 0.046 (**Figure 3b**). Uniformity and reproducibility of OAc-IONPs are indispensable requirements for approval of FDA and we successfully synthesized homogeneous OAc-IONPs that have small size variation in six different batches.

It is necessary to go through the surface modification step of the initial OAc-IONPs with hydrophilic ligand in order to apply them to the biomedical environment because the OAc-IONPs are dispersed only in the organic solvent such as hexane or chloroform. Therefore, we designed and synthesized the surface coating materials via RAFT polymerization method which have multidentate anchoring groups and hydrophilic groups to improve colloidal stability and hydrophilic property of the OAc-IONPs. The RAFT polymerization method has the following advantages: (1) Easy introduction of various functional groups based on the same backbone moiety just depending on the type of monomers used in the polymerization. (2) Control of the composition and molecular weight of polymers as desired. (3) Synthesis of polymers with narrow polydispersity.

The synthesized ligands were composed of three groups: anchoring group, hydrophilic group, and functional group. Catechol-derived dopamine was used as an anchoring group, which could coordinate with the surface of IONPs. The functional group was used to give different charges. Carboxyl group (acrylic acid) was used as a negative charge and tertiary amine group (N-[3-(Dimethylamino)propyl] acrylamide)) was used as the positive charge. As a hydrophilic group, a substance containing PEG was used because the hydrophilic property of PEG improves the dispersibility of IONPs in aqueous solution. In general, PEG has several advantages such as increasing biocompatibility, reducing immunogenicity, and providing stability between particles via steric repulsion.[41] It also reduces the adsorption of various plasma proteins[42] and enables the circulation in the body for a long time *in vivo*. Therefore, PEG is one of the ideal coating materials.[43-44] Prior to synthesis of charged ligands, we tested whether RAFT polymerization system could work successfully in the synthesis of (n) ligand. Molecular weight of polymer was well controlled by using RAFT agent. In case of using the RAFT agent, the PDI value was

1.19 although the PDI was 1.79 without RAFT agent (**Figure 4a**). Also, degree of polymerization (DP) of the (n) ligand was increased as the [Monomer]:[RAFT] ratio increase, although there was a difference between the theoretical [Monomer]:[RAFT] ratio and the measured degree of polymerization (DP) of the (n) ligand analyzed by GPC (in **Figure 4b**). We presupposed that this result could be caused by catechol group which could be used as radical scavenger. Also, we confirmed that well controllable polymerization of (n) ligand. It was possible to control of the monomer ratio in polymer by RAFT polymerization method. [DMA]:[PEG] ratio in polymer were well controlled as desired. In **Figure 5**, calculated ratio of DMA to PEG in (n) ligand measured by ^{1}H NMR was corresponded approximately to theoretical ratio as we desired. Based on these results, three charged ligand were synthesized. We designed the final polymer composition with 20% of anchoring groups (DMA), 50% of hydrophilic groups (PEG moieties), and 30% of neutral groups, negatively or positively charged functional groups for charged IONPs respectively (**Figure 6a**). The reason of the polymer design was that dispersity of the nanoparticles in the cell culture media was remarkably decreased in the case of the ligand composed of 20% of the anchoring group and 80% of the functional group without the PEG part although the nanoparticles were well dispersed in the aqueous solution (**Figure 7**). It was confirmed that each monomer was polymerized at a desired ratio by the ^{1}H NMR spectra as shown in **Figure 6b.** Each proton peak of DMA, PEG, and tertiary amine was observed at 6.5~6.8 ppm, 3.64 ppm, and 2.25 ppm by ^{1}H NMR spectroscopy, respectively. The (n) ligand was functionalized with 18% of the anchoring group and 82% of the hydrophilic group. In the case of the (+) ligand, the anchoring group was 18%, the hydrophilic group was 49% and the quaternary amine functional group was 31%. In the case of the (-) ligand, the ratio of anchoring and hydrophilic groups were identical to the (+) ligand so we expect the monomer ratio of (-) ligand. Molecular weight of (-) ligand, (n) ligand, (+) ligand was 6741 (PDI = 1.28), 9122 (PDI = 1.29), 3144 (PDI = 1.25) respectively, and the PDI values of all the ligands were low (PDI < 1.3).
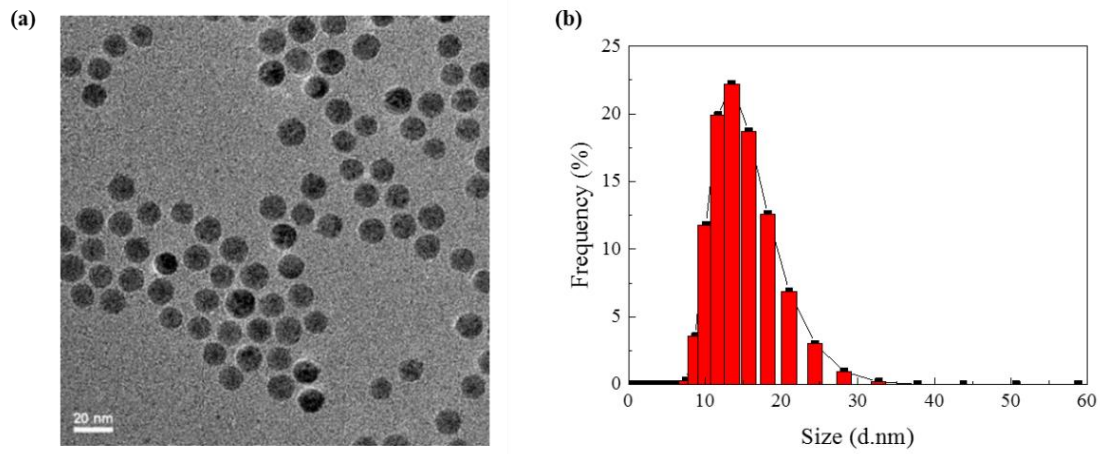
Figure 3. Synthesis of OAc-IONPs. (a) TEM image and (b) H.D of OAc-IONPs of dispersed in hexane measured by DLS.
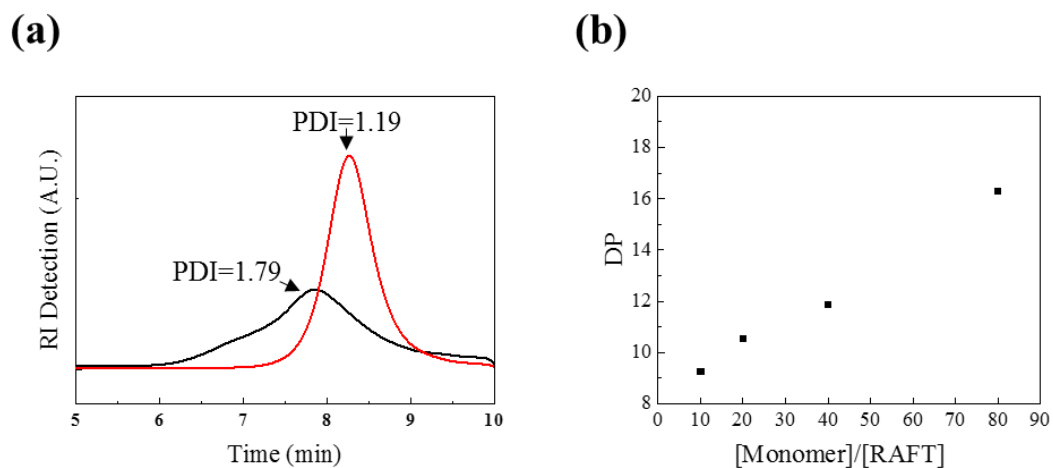
Figure 4. RAFT polymerization of (n) ligand. (a) Result of GPC analysis of (n) ligand in THF, showing narrow PDI with a [Monomer]:[RAFT] ratio of 20:1 and [AIBN]:[RAFT] ratio of 1:1 (red line), and poor PDI without RAFT agent (black line). (b) Controllable polymer DP as a [Monomer] to [RAFT] ratio.
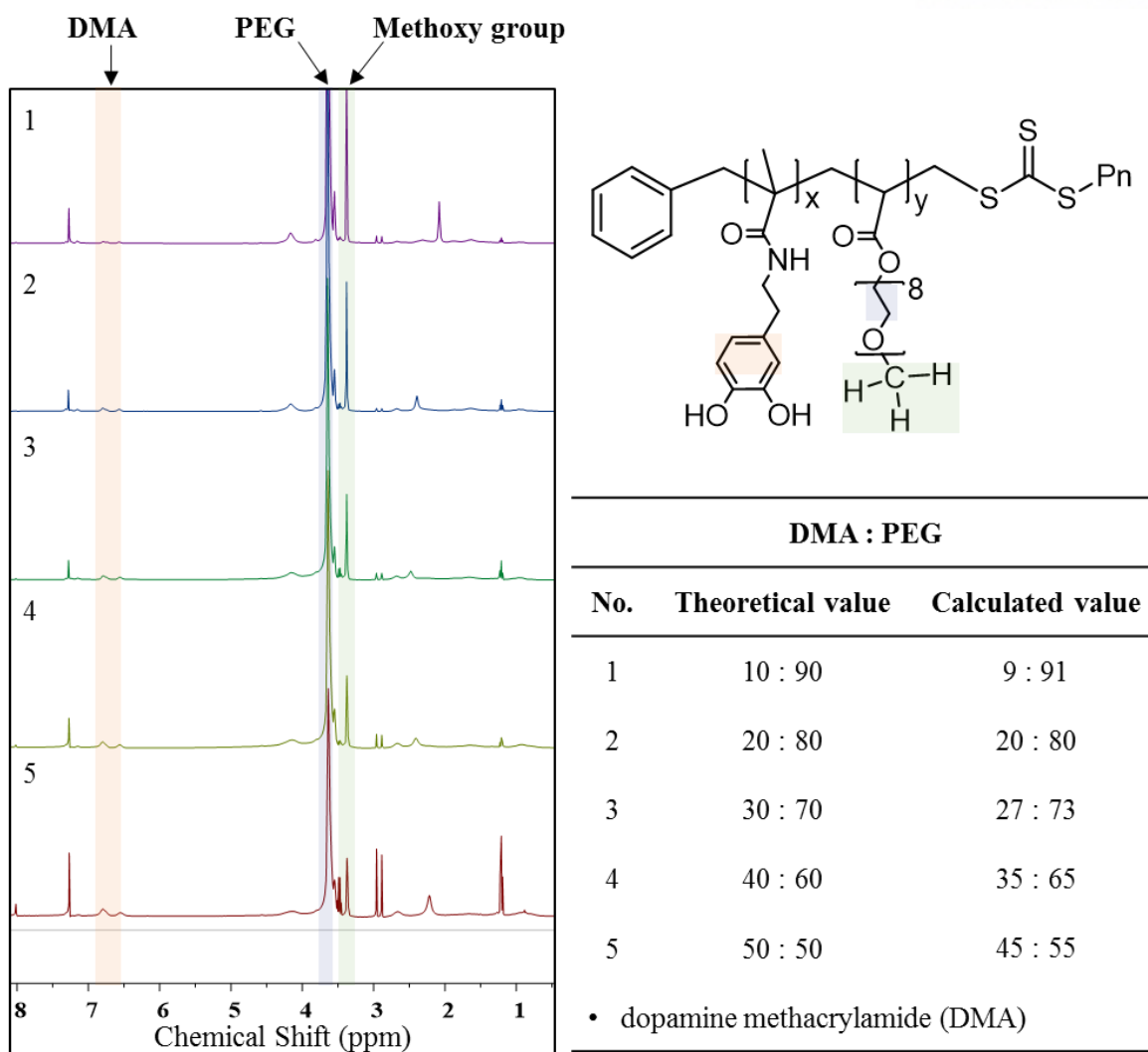
Figure 5. Control of monomer ratio in polymers. Result of ^{1}H-NMR analysis.

	DMA : PEG	
No.	Theoretical value	Calculated value
1	10 : 90	9 : 91
2	20 : 80	20 : 80
3	30 : 70	27 : 73
4	40 : 60	35 : 65
5	50 : 50	45 : 55

- dopamine methacrylamide (DMA)

(a)

(b)

Ligand type	Anchor group	Hydrophilic group	Functional group
(−) ligand	19%	50%	31%
(n) ligand	18%	82%	0%
(+) ligand	19%	50%	31%
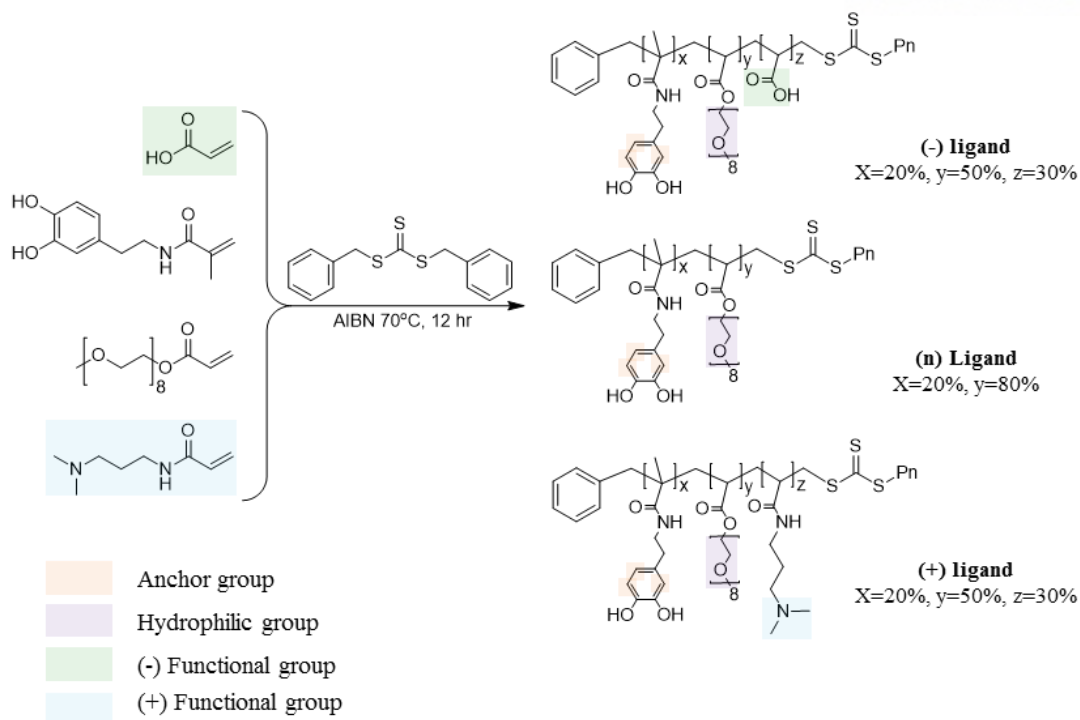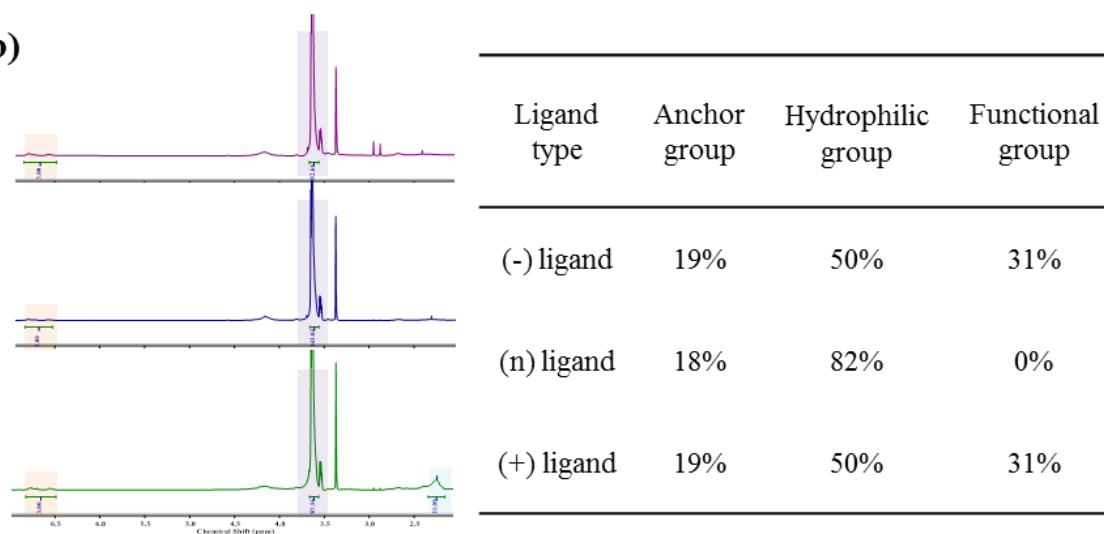
Figure 6. RAFT polymerization reaction for synthesis of different charged polymer ligands. (a) Scheme of ligand synthesis, and (b) ^{1}H-NMR analysis of charged ligands in CDCl$_3$.
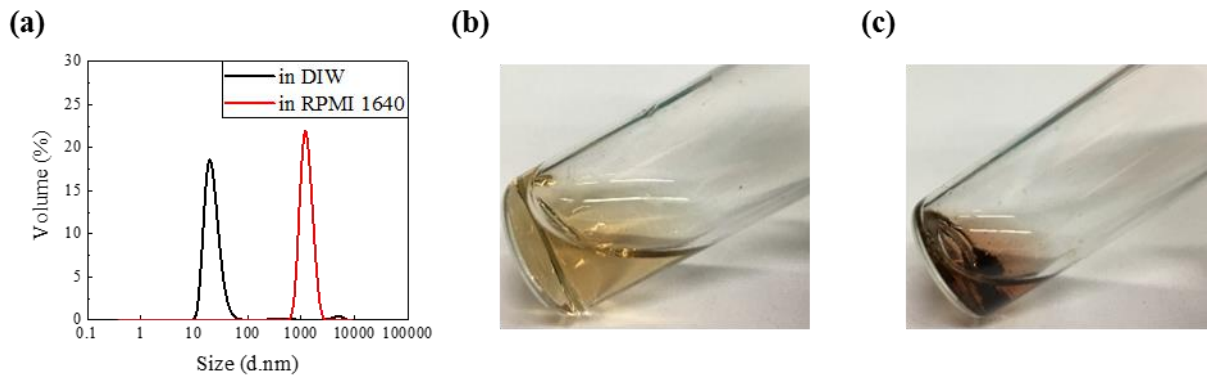
Figure 7. Stability test of 80% positively charged IONPs. (a) H.D of 80% positively charged IONP dispersed in DIW and RPMI 1640 media. (b) Camera image of the IONPs dispersed in DIW, and (c) agglomerated in RPMI 1640 media.

2.3.2 Ligand Exchange of IONPs for Dispersing in the Aqueous Solution. After the synthesis of ligands, we did a ligand exchange to convert the hydrophobic material initially synthesized in the organic solvent into a water-dispersible hydrophilic material as shown in **Figure 8a**. The ligand exchange has the advantage of simply compacting ligands without significantly increasing of H.D. It is very important to coat the surface uniformly and compactly for the accurate analysis of surface characteristics and reproducible synthesis of IONPs. We could also obtain a consistent toxicity evaluation value under the proposed ligand exchange method. As shown in **Figure 8b**, the uniform distribution of OAc-IONPs (about 11.6 ± 0.7 nm) and surface-modified three IONPs were observed by TEM. The H.D of OAc-IONPs was also uniformed about 14.58 nm and PDI value was 0.046. Also, synthesized compact and uniform IONPs showed no big change of the H.D between OAc-IONPs and three charged IONPs (**Figure 8c**). The PDI values of them were low (0.25-0.3). The surface charge of each charged IONPs was measured by zeta-potential as shown in **Figure 8d**. The surface charge of (-) IONPs, (n) IONPs, and (+) IONPs was -39 mV, -0.6 mV, and +32 mV, respectively. As a result, three different charged IONPs were successfully synthesized.
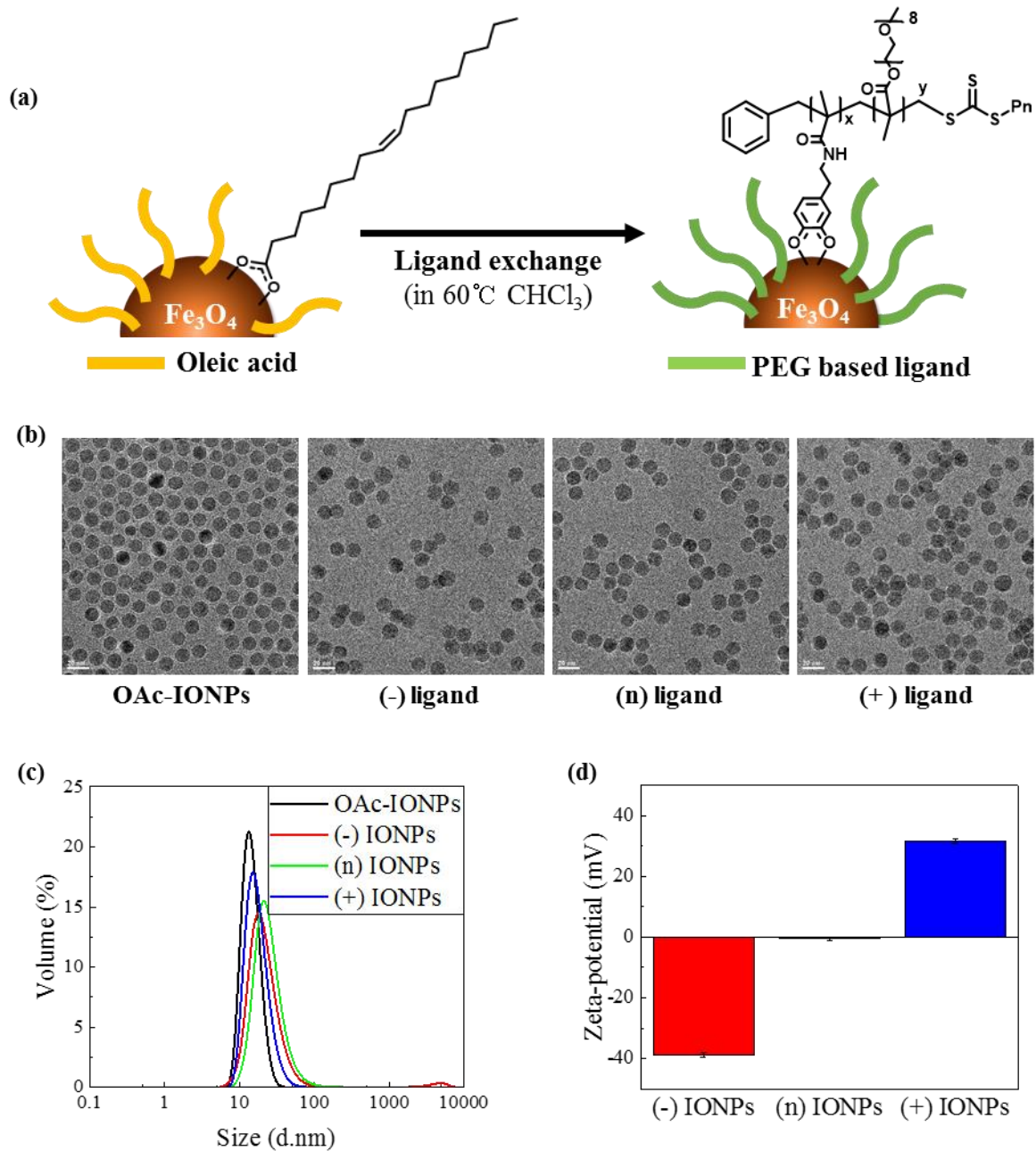
Figure 8. Characterization of IONPs after the ligand exchange. (a) Schematic illustration of ligand exchange of OAc-IONPs with charged ligands, (b) TEM images of OAc-IONPs dispersed in hexane and three charged IONPs dispersed in DIW. (c) H.D of OAc-IONPs and the three charged IONPs, and (d) zeta-potential of three charge IONPs.

2.3.3 Stability of IONP in DIW and Cell Culture Media. It is important to provide the stable nanoparticles with the properties of the material maintained in an aqueous condition. Although the synthesized nanoparticles have initial colloidal stability, they may become unstable due to the changes in physical properties depending on the storage period and the storage method, which affects the toxicity of IONPs. Therefore, we tested the stability of IONPs by storing IONPs in DIW at 4°C refrigerator for three months after sealing them with a parafilm and wrapping them in the foil and by measuring DLS and zeta-potential value of IONPs. In **Figure 9a**, the H.D of the (-) IONPs and the (n) IONPs shows a very subtle increase in the DIW. The change of H.D of the (-) IONPs and (n) IONPs was ± 5.36 nm and ± 4.98 nm over the three months, respectively. Moreover, the (+) IONP remained constant at ± 1.57 nm with almost no change in size. In **Figure 9b**, the zeta-potential value of (-) IONPs, (n) IONPs, and (+) IONPs was ± 6.24 mV, ± 2.31 mV, and ± 4.77 mV respectively. Notably all the synthesized IONPs with polymer ligands show high stability in their size and surface charge.

We further studied the stability of IONPs in the cell culture media where there are a lot of factors affecting the physi-co-chemical properties of nanomaterials such as proteins, salts, and various pH conditions. We used RPMI 1640 media and DMEM media to find out the stability of the IONPs for two days and then analyzed the H.D by DLS as shown in **Figure 9c** and **Figure 9d**. In general, charged substances tend to aggregate or form protein corona in media.[45] However, all of our charged IONPs showed no change in their size for two days in both RPMI 1640 and DMEM media. This means that all of the differently charged IONPs were stable enough to conduct *in vitro* test to fulfill the requirements of the same condition as above. The origin of the high stability of IONPs is from robust binding affinity between catechol and iron ion owing to multi-anchor group. In addition, introducing the PEG moiety and adequate charged group to surface of IONPs also endow optimized NP stability via combination of steric hindrance and charge-charge repulsion. Therefore, we could make an accurate toxic evaluation system with three kinds of charged IONPs with minimizing the variable factors derived from material property which would be addressed in the next section.
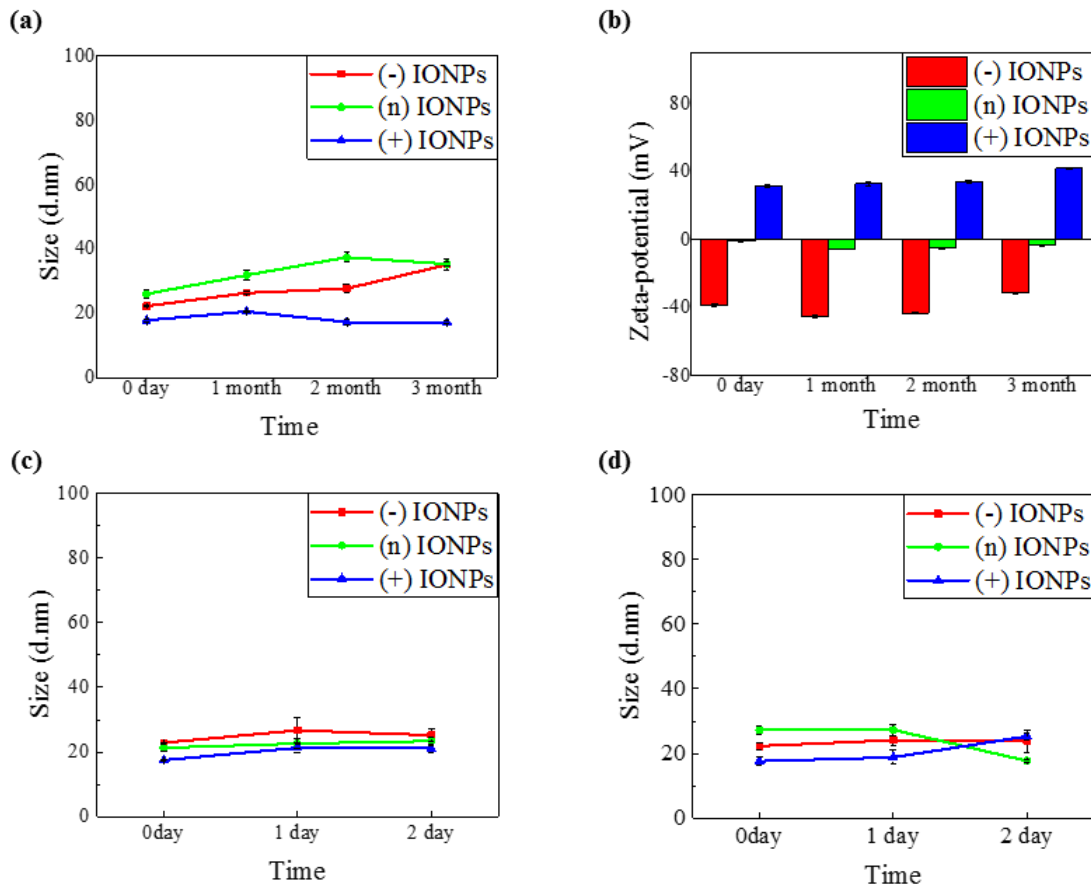
Figure 9. Colloidal stability of three charged IONPs in DIW for three months and cell culture media for two days. (a) H.D and (b) zeta-potential of three charged IONPs in water for three months. H.D of three charged IONPs (c) in RPMI1640 media and (d) in DMEM media for two days.

2.3.4 Cell Viability and Morphological alteration on the Cells. To determine if the surface charge of IONPs influences the cytotoxicity of IONPs, we conducted an MTT assay in the three human cell lines.[46] A549 (human lung cancer cell), Huh-7 (human liver cancer cell), and SH-SY5Y (human neural cancer cell) were used as the cell lines to confirm the cytotoxicity of different three target organs such as lung, liver, and nerve against external substances.[47] After each cell was treated with various concentration (0, 2, 8, 31, 125, and 500 µg Fe/mL) of each differently charged IONPs for 24 h, the adsorption of formazan was measured at 560 nm as shown in **Figure 10.** In each cell line, all of the IONPs showed the similar tendency of cell viability. The viability showed a slightly decrease depending on concentration of IONPs. It is generally known that positively charged nanoparticles are more uptaken because of electronic interaction with the cell membrane, which consequently leads to a serious toxicity. However, in our study, all of the three IONPs showed low toxicity even if it was treated with 500 µg Fe/mL.

To verify the effect of IONPs on cell morphology, we confirmed cell morphology with differently charged IONPs by microscopy in each cells at two concentration of 10 µg Fe /mL and 100 µg Fe/mL as shown in **Figure 11**. It was confirmed that morphology alteration in A549, Huh-7, and SH-SY5Y cells was not observed up to high concentration compared to the control group. Based on the MTT assay and observation of cell morphology, we could conclude that there was no cytotoxicity in our charged IONPs.
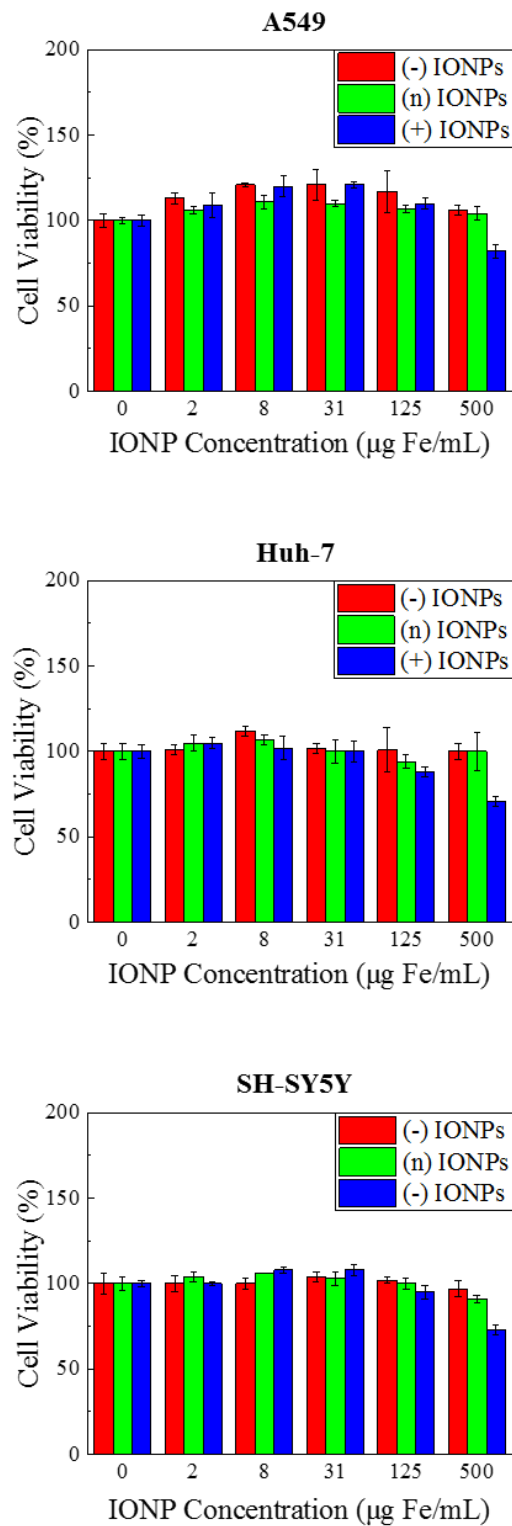
Figure 10. Effect of the three charged IONPs on the viability of three different cells; A549, Huh-7, SH-SY5Y cells. All cells were exposed for 24 h to increasing concentrations upon 500 µg Fe/mL. Cell viability was analyzed by MTT assay.
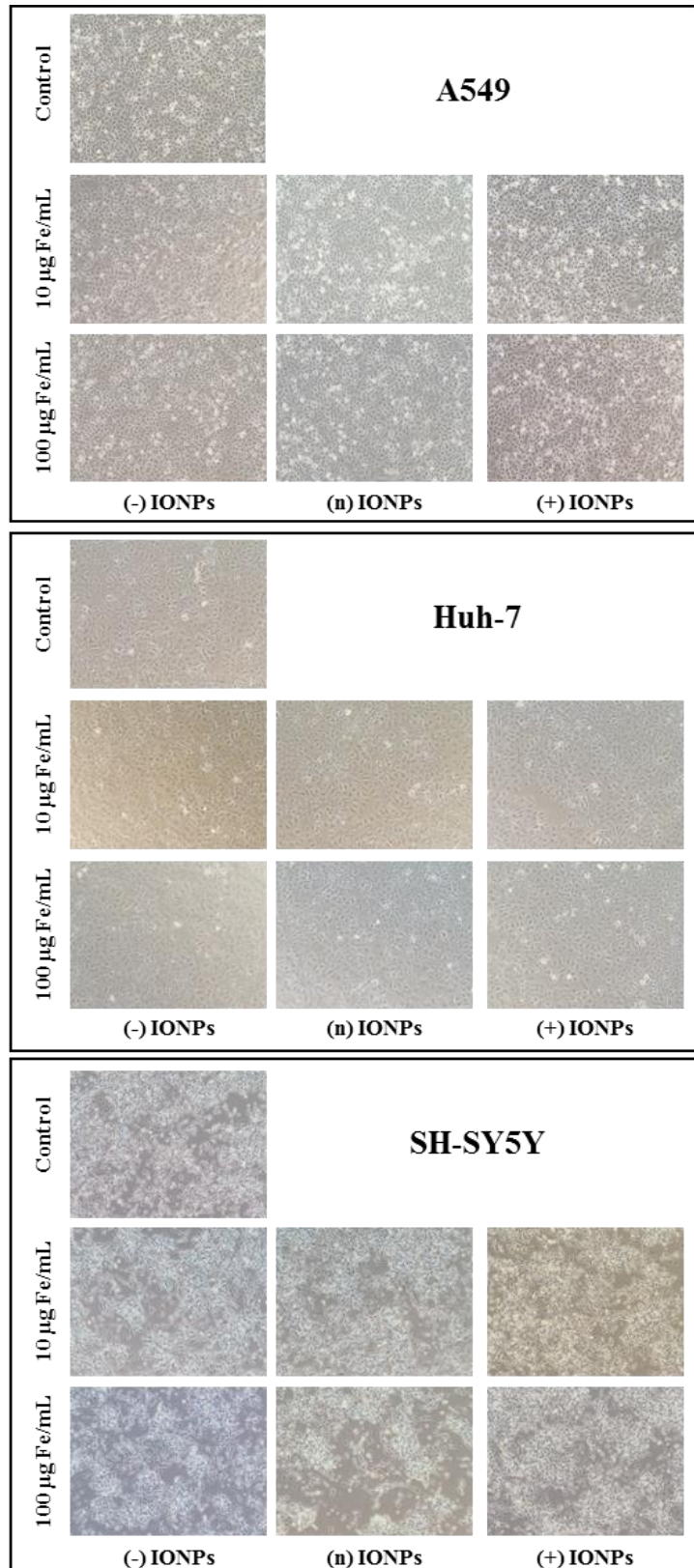
Figure 11. Cell morphological alteration in A549, Huh-7, and SHSY-5Y after treatment of three IONPs with 10 and 100 μg Fe/mL by microscopy.

2.3.5 Hematological and Histological Toxicity in Mice. To observe the *in vivo* toxicity of three different charged IONPs in mice, we conducted hematological and histological analysis. The three differently charged IONPs were treated in mice at 2 µg Fe/g and 10 µg Fe/g for 24 h via intravenous injection respectively. In the hematological analysis, we tested following parameter: BUN and CREA associated with the kidney function and ALT, ALP, AST, and TBIL associated with the liver function. All the three IONPs showed no significant changes in all blood parameters compared to negative control (**Figure 12**).

A histological examination was also performed and six organs were observed; liver, kidney, lung, heart, spleen and brain which were rated from level 0 to level 5. The (-) IONPs and (+) IONPs showed weak toxicity equivalent to level 1 in kidney and heart, respectively. Although the (n) IONPs showed toxicity of level 1 and 2 depend on concentration in both liver and kidney, it was not a serious toxicity such as necrosis. The (n) IONPs showed higher toxicity level than (-) IONPs and (+) IONPs because the (n) IONPs has more PEG moiety than other two IONPs. These results are consistent with reported studies to be related side effects of the PEGylation.[48] However, all the synthesized IONPs showed no significant toxicity *in vivo* test such as necrosis or accurate toxicity (**Figure 13**). These results indicate that charged IONPs can apply to various biomedical field as biocompatible materials by controlling the surface ligand and depending on usage.
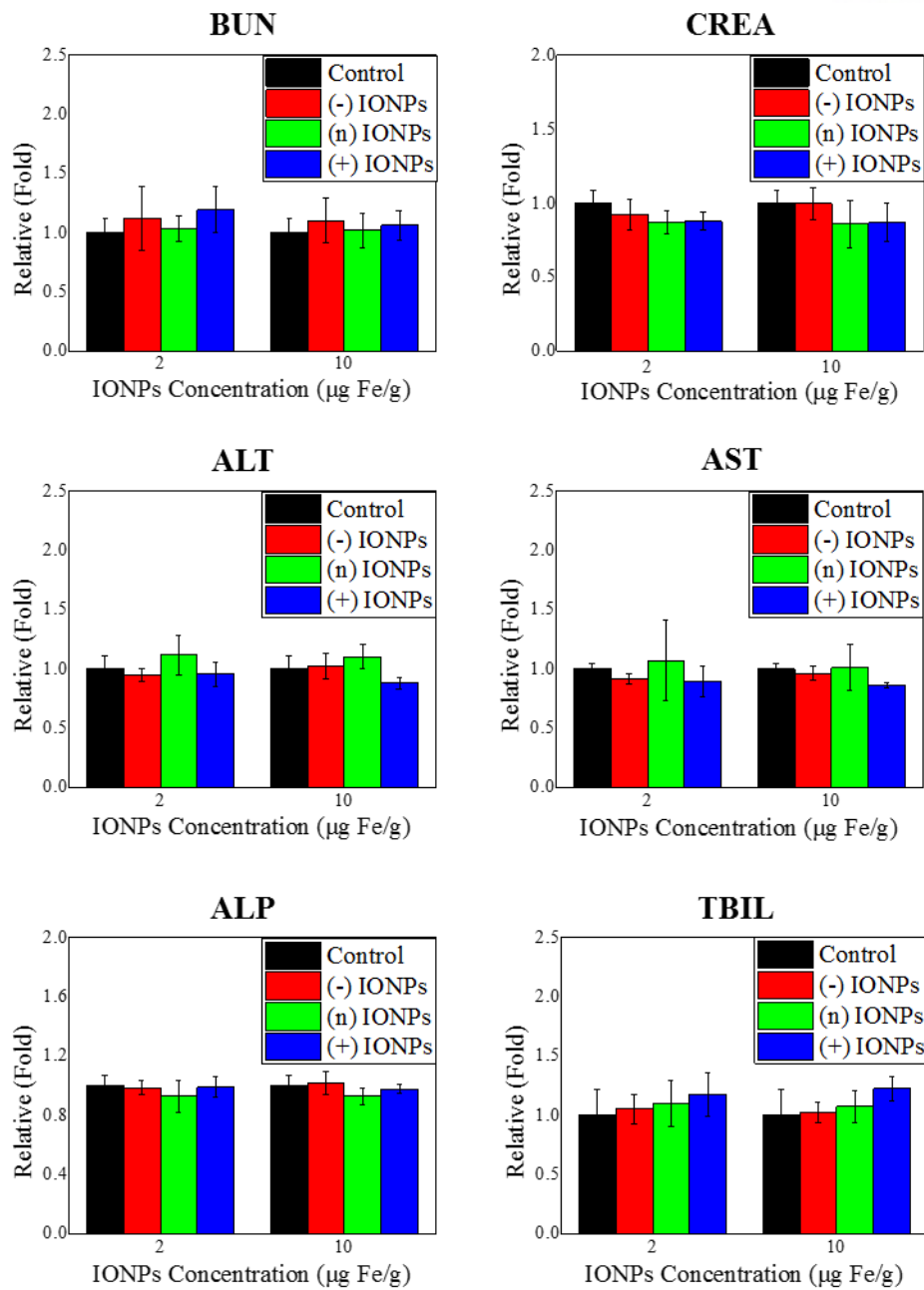
Figure 12. Hematological analysis of balb/c mice following injection of three charged IONPs. The graphs show the concentration of BUN, CREA, AST, ALT, ALP, and TBIL of mice after intravenous injection with the charged IONPs (2 μg/g and 10 μg/g) for 24 h. ($n = 3$)

	Control (1X PBS)	(-) IONPs		(n) IONPs		(+) IONPs	
IONPs / Tissue		2 µg Fe/mL	10 µg Fe/mL	2 µg Fe/mL	10 µg Fe/mL	2 µg Fe/mL	10 µg Fe/mL
Kidney[1]		▪	▪	▪			
Kidney[2]		▪		▪			
Kidney[3]					▪		
Liver[2]					▪		
Lung							
Heart[4]						▪	
Spleen							
Brain							

1) Basophilic tubules 2) Inflammatory cell foci 3) Mineralization 4) Cardiomyopathy

Toxicity levels from 0 to 5
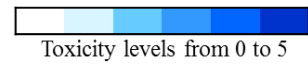
Figure 13. Histological analysis of balb/c mice after exposure of three charged IONPs (2 µg/g and 10 µg/g) for 24 hr in six organs; kidney, liver, lung, heart, spleen, and brain. Toxicity level rated from 0 to 5. ($n = 3$)

2.4 Conclusions

We successfully developed the three differently charged IONPs for high colloidal stability and performed a systematic evaluation of cytotoxicity in the three human cell lines-A549, Huh-7, and SH-SY5Y. Through RAFT polymerization and ligand exchange method, we prepared three differently charged IONPs with DMA as multiple anchoring groups, hydrophilic PEG polymer, negative carboxylic acid, and positive quaternary amine. All of the charged IONPs showed monodispersion with narrow size distribution in aqueous solution and high colloidal stability for up to three months in DIW and two days in RPMI 1640 and DMEM cell culture media without agglomeration. Depending on the concentration of IONPs, toxicity was assessed *in vitro* in three cell lines (lung, liver, and brain) by investigating cell viability test, morphology change. In MTT assay, all of the charged IONPs showed no significant toxicity in each cells up to the maximum concentration of 500 µg Fe/mL, and there was also no critical damage of cell morphology in all each cells. *In vivo* test, we performed hematological and histological analysis in mice and the results showed that the three differently charged IONPs are non-toxic and biocompatible materials. These results suggest that the charged IONPs with high stability and low toxicity in physiological conditions have potential for application at various bio-medical field.

III. Multidentate Catechol-Based Zwitterionic Ligand for Excellent Stability and Bio-Functionalization to Iron Oxide Nanoparticles

3.1. Introduction

IONPs have been studied in various bio-application such as MRI contrast agent,[49] drug delivery,[50] and hyperthermia[51] because they have unique properties such as superparamagnetism, low toxicity, and easy surface modification.[52] High-quality IONPs synthesized by thermal decomposition method in hot surfactant solution are required for additional surface modification process to render the IONPs biocompatibility because initial IONPs have hydrophobic ligands. In general, surface of the IONPs should meet the following requirements for bio-application; i) high colloidal stability in wide pH ranges and saline solutions, ii) compact and uniform H.D, iii) reduced nonspecific binding with proteins of biological media, and iv) easy functionalization to biomolecules.

For the various biomedical application, it is important to do surface engineering of IONP for the functionalization. There are two main reliable approaches for biocompatible and bio-functional surface of IONPs such as encapsulation and ligand exchange. Encapsulation can preserve the native ligands and maintain the physical properties, but it tends to increase the H.D of the final hydrophilic nanoparticles.[53] Ligand exchange can replace the hydrophobic shell on IONPs with biocompatible ligands, which consist of anchoring groups, hydrophilic groups, and functional groups. Ligand can be composed of anchoring group for binding onto the surface of the IONPs, hydrophilic group for dispersity in water such as PEG and zwitters, and other functional groups for conjugation of bio-molecules. Catechol has been used as anchoriong group for binding onto the IONPs because it exhibits strong affinity to metal oxide nanoparticles such as iron oxide, titanium oxide, alunium oxide.[54] PEG has been well known for stealth materials as hydrophilic molecules because it has good water solubility, colloidal stability, and long-term circulation time in vivo. In addition, multidentate anchoring groups improve colloidal stability of the IONPs in biological media by enhancing the affinity of ligands with the surface of IONPs, while monodentate anchoring groups which have weak binding affinity with the IONPs surface. Therefore, multidentate catechol-based PEG ligand systems and have been studied for surface coating of IONPs for high stability and biocompatibility.[55] However, previous PEG-based IONPs have had limitations such as increasing H.D of IONPs, and being unstable in acidic or high saline buffer resulting in aggregation. These limitations can prevent renal excretion and cause the accumulation in organs.[56]

Recently, several research groups have reported zwitterionic materials to overcome these limitations of PEG. Zwitterionic ligands containing both positive and negative charge groups in one molecule have zero net charge. They provide strong hydration that can capsulate the NPs and prevent aggregation and excellent resistance to nonspecific protein adsorption owing to their highly dense and zero net charge.[57-58] The IONPs coated with zwitterionic polymer with multiple anchoring groups have been little studied so far, as well as have been not applied to quntum dots,[59-60] gold nanoparticles[61] and silver nanoparticle[62] athough there have been studies about development of low-molecular weight zwitterionic coating materials including sulfobetaine,[37] carboxybetaine,[63] phosphorylcholine,[64] and poly(acrylic) aicd.[65]

In this study, we have developed a new multidentate catechol-based zwitterionic ligand (MCZ-ligand) system in order to increase the colloidal stability of IONPs. MCZ-ligand was synthesized by RAFT polymerization which offers the ability to control properties of polymer as desired by varying composition and ratio of monomers. Hydrophobic ligand of initally synthesized IONPs was replaced with the MCZ-ligand by simple coating method one step and the MCZ-ligand coated IONPs (MCZ-IONPs) was well dispersed in water uniformly and compactly, and MCZ-IONPs showed excellent colloidal stability and was able to easily introduce bio-functional groups.

3.2 Materials and Experimental Section

3.2.1 Materials. [3-(Methacryloylamino)propyl]dimethyl(3-sulfopropyl)ammonium hydroxide inner salt (ZMA), 2-Carboxyethyl acrylate, 2-Cyano-2-propyl benzodithioate, 4,4'-Azobis(4-cyanovaleric acid), Bis(hexamethylene)triamine, N-(3-Dimethylaminopropyl)-N′-ethylcarbodiimide hydrochloride (EDC) were purchased from Sigma Aldrich. 2,2,2-Trifluoroethanol were purchased from Alfa-Aesar and N-Hydroxysulfosuccinimide sodium salt (sulfo-NHS) were purchased from TCI. 1X PBS, 1 M MES buffer were purchased from Biosesang. DMA and biotinylated methacrylate were synthesized as above procedures.

3.2.2 Synthesis of OAc-IONPs. 12 nm sized OAc-IONPs were synthesized by using a previously described thermal decomposition method in the high boiling solvent.[40] Synthesized OAc-IONPs were analyzed by TEM (JEOL, JEM-2100F).

3.2.3 Synthesis of MCZ-Ligand. We synthesized MCZ-ligand by RAFT polymerization method. Polymer was composed of 20% DMA as anchoring groups and 80% ZMA as hydrophilic groups. First, DMA (0.2 mmol), 2-Cyano-2-propyl benzodithioate (0.05 mmol), 4,4'-Azobis(4-cyanovaleric acid) (0.05 mmol) were dissolved in 250 μL methanol, and ZMA (0.8 mmol) was dissolved in 750 μL 2,2,2-Trifluoroethanol. Two solutions were mixed and transferred to 5 mL ampule. After 4 cycles of freeze-pump-thaw, the ampule was sealed by using a torch under vacuo. The mixture was heated to 70°C and reacted for overnight. After reaction, the excess residues were washed with 2,2,2-Trifluoroethanol and acetone by centrifugation. We repeated this washing process three times and solvent was removed in vacuo to obtain the final polymer products. Synthesized polymers were confirmed by ^{1}H NMR using AVANCE III HD (Bruker) instrument at 400 MHz using deuterium oxide solution. Molecular weight and molecular weight distribution were determined by GPC (Agilent).

3.2.4 Surface Modification of OAc-IONPs via Ligand Exchange Method. OAc-IONPs (10 mg) were dissolved in 400 μL CHCl$_3$, MCZ-ligand (30 mg) was dissolved in 200 μL 2, 2, 2-Trifluoroethanol. Two solutions were mixed in 10 m L vial and added 200 μL DIW. The vial was heat to 60°C and reacted for 12 h. After the reaction, the solution was precipitated in acetone by centrifugation (3 min, 3000 rpm) and the precipitates were dissolved in DIW. To remove the excess reagent, we used a centrifugal filter (MWCO 50 k) and washed out in DIW and repeated three times. Final MCZ-IONPs were stored in DIW.

3.2.5 Stability Test of IONPs in Various pH Solutions and Saline Solutions. Different pH buffer solutions (pH 3, 5, 7, 9, 11) and various concentration of sodium chloride solution (0.1 M, 1 M, 2 M) were prepared and 12 nm MCZ-IONPs were added to each buffer solution. Final concentration of the

IONPs sample was 3 mM. The H.D of the IONPs was measured using a DLS (Malvern Zetasizer Nano-ZS90) equipped with a detection angle fixed at 90˚ degrees and laser wavelength providing at 633 nm.

3.2.6 Protein Adsorption Test. 0.05 μM MCZ-IONPs were mixed with various concentration bovine serum albumin (BSA) in 1X PBS. After incubation for 30 min, we measured H.D of IONPs by DLS.

3.2.7 Synthesis of Amine Linked Biotinylated IONPs. First, we synthesized carboxylated zwitterionic ligand according to the same way as described above except for the addition 2-carboxyethyl acrylate. Next, OAc-IONPs were coated with the carboxylated zwitterionic ligand as according to described method above. For synthesis of amine functionalized IONPs, we used diamine linker; Bis(hexamethylene)triamine. In carboxylated zwitterionic coated IONPs solution (0.1 nmol), EDC (1 μmol) and sulfo-NHS (0.5 μmol) were added and the mixtures were reacted in 10 mM MES buffer (pH 6). After for 30 min, Bis(hexamethylene)triamine (1.2 μmol) was added the solution which was pH 8 solution made by 0.5 M sodium carbonate buffer. Final volume of mixtures was 500 μL. Finally, amine linked biotinylated IONPs (AB-IONPs) were synthesized. Biotin (1 μmol) was dissolved in DMSO, and the biotin solution, EDC (1.2 μmol), and sulfo-NHS (0.6 μmol) were added the biotin solution. After 30 min, amine functionalized IONPs were mixed with the biotin solution, and the mixture was reacted for 12 h in sodium phosphate buffer solution (pH 8). After reaction, excess reagents were removed by centrifugal filter (MWCO 50 k) with three times. Final AB-IONPs were stored in DIW.

3.2.8 Synthesis of Direct Biotinylated IONPs. For synthesis of direct biotinylated IONPs (DB-IONPs), first biotinylated methacrylate were synthesized as previously report.[37] After that, biotinylated zwitterionic polymer was synthesized by using DMA, ZMA, and biotinylated methacrylate. OAc-IONPs were coated with the biotinylated zwitterionic polymers via same ligand exchange method as described above. Then, final DB-IONPs were obtained.

3.2.9 Interaction Between Biotinylated IONPs and Streptavidin Solution. After synthesis of AB-IONPs and DB-IONPs, the 0.01 μM biotinylated IONPs were incubated with various concentration of streptavidin solution dispersed in 1X PBS for 30 min at room temperature. After incubation, the H.D of IONPs solution was measured by DLS.

3.2.10 Streptavidin Conjugation on IONPs. In carboxylated zwitterionic IONPs solution (0.1 nmol), EDC (1 μmol) and sulfo-NHS (0.5 μmol) were added and reacted in 10 mM MES buffer (pH 6). After for 30 min, streptavidin solution dispersed in 1X PBS (0.5 nmol) was added the IONPs solution which was pH 8 solution made by 0.5 M sodium carbonate buffer. Final volume of mixtures was 1500 μL, and the mixtures were reacted for 12 h in pH 8 buffer solution. After reaction, excess reagents were removed by spin-down repeated 3 times at 15000 rpm for 30 min with 1X PBS. The final streptavidin conjugated IONPs (SA-IONPs) were stored at 1X PBS.

3.2.11 Interaction Between SA-IONPs and Biotin-Coated Silicon Glass. For specific interaction of SA-IONPs with biotinylated silicon glass, we prepared both the (3-Aminopropyl)trimethoxysilane (APTMS) coated silicon glass as control group and biotinylated silicon glass. First, the oxygen plasma was treated on both side of silicone materials, and put the silicone materials into the APTMS solution (0.5 % of APTMS in acetonitrile, v/v) for 1 h at room temperature. After that, the materials were washed with acetonitrile and methanol, and dried via nitrogen blowing. For coupling of biotin on to the APTMS coated silicon glass, the APTMS coated glass was placed in a mixture of 10 mM biotin, 10 mM HATU and 20 mM DIPEA in N,N-Dimethylformamide for 2 h, and excess biotin was washed with N,N-Dimethylformamide and methanol. After that, the glass was dried using nitrogen gas. SA-IONPs were treated on the APTMS coated silicon glass and biotin coated silicon glass, and the glass were analyzed by scanning electron microscope (SEM) and Energy-dispersive X-ray spectroscopy (EDX) analysis.

3.3 Result and Discussion

3.3.1 Synthesis and Characterization of MCZ-Ligand

MCZ-ligand was synthesized by RAFT polymerization. The chemical synthetic scheme of MCZ-ligand are showed in **Figure 14a**. The MCZ-ligands were composed of followed by three groups; anchoring groups, hydrophilic groups, and functional groups. Sulfobetaine group of zwitterionic monomer was introduced for reduce nonspecific protein adsorption.[56] 2-Cyano-2-propyl benzodithioate and 4,4'-Azobis(4-cyanovaleric Acid) were used as RAFT agent and inhibition with ratio of 1:1. To optimize polymerization condition, we varied some parameters such as solvent, polymerization time. First, we optimized solvents condition by using N, N-Dimethylformamide, methanol, water, and 2,2,2-Trifluoroethanol to solve the problem of precipitation during the polymerization due to the different solubility of two monomers. The polymer was synthesized uniformly without precipitation in the combination of methanol and 2,2,2-Trifluoroethanol (no data). Next, polymer was synthesized depending on time; 3 h, 9h, and 18 h. The molecular weight was increased depending on time although there was a little difference at 9 h and 18 h. Therefore, polymerization time was optimized to 12 h.

A ratio of 20% DMA and 80% ZMA was reacted and the final product was analyzed by ^{1}H NMR analysis (**Figure 14b**). The calculated ratio was 17% of DMA and 83% of ZMA in polymer and it was similar to what we intended. GPC analysis showed a single peak and uniform molecular weight of 23,400 (PDI = 1.26).

(a)

(b)
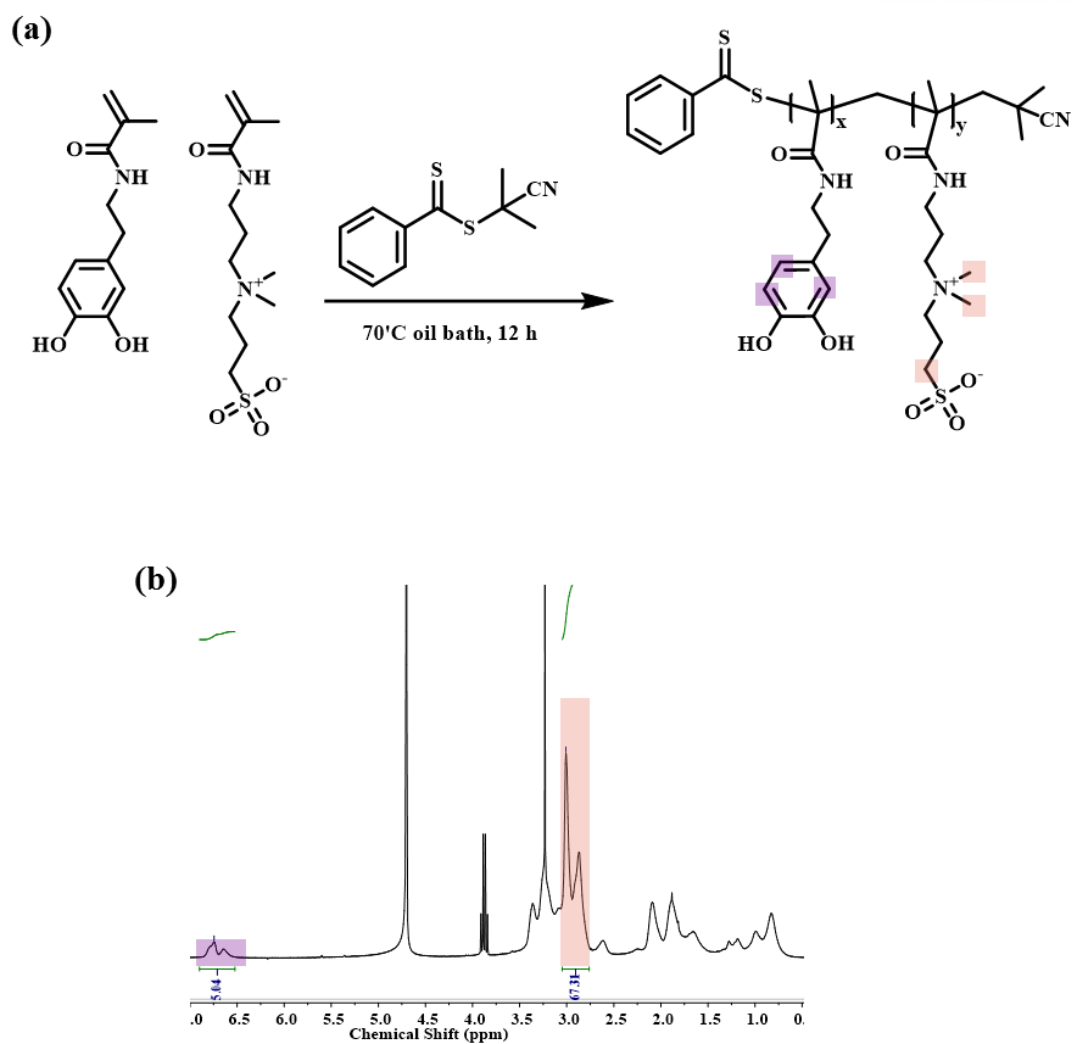
Figure 14. Synthesis and characterization of MCZ-ligand. (a) Scheme of MCZ-ligand synthesis, and (b) ^{1}H NMR analysis of MCZ-ligand in D_2O.

3.3.2 Surface Modification of IONPs and Characterization

Many previous reports processed two step for surface ligand exchange of IONPs because MCZ-ligand has strong hydrophilic properties and it is very difficult to modify.[66] The first step is transferring particles to relative hydrophilic organic solvent and the second step is transferring them to aqueous solution, which is complex and cumbersome. Therefore, we optimized ligand exchange method for one step method. **Figure 15a** shows scheme of ligand exchange. There are two system, one is one-phase system which uses chloroform, TFE, and water combination, and the other is two-phage system which uses hexane and water. The one-phase system was able to compactly and homogeneously modify, while the heterogeneous H.D of the MCZ-IONPs was shown in two-phase system. It is considered that the IONPs and the MCZ-ligand could not be collided and well separated in the hexane and water solutions because the MCZ-ligand is strong hydrophilic. In the one-phase system, the OAc-IONPs were modified to MCZ-IONPs uniformly and compactly, and OAc-IONPs dispersed in hexane were transferred to DIW (**Figure 15b**). The H.D of MCZ-IONPs was about 20 nm and a little increased compared to OAc-IONPs (**Figure 15c**). The zeta-potential of MCZ-IONPs was about -20 mV. We presumed that weakly negatively charged zeta-potential could be caused by terminal sulfone group of MCZ-ligand (**Figure 15d**). PEGylated IONPs were prepared as a control group for comparing MCZ-IONPs in next colloidal stability and nonspecific binding test.
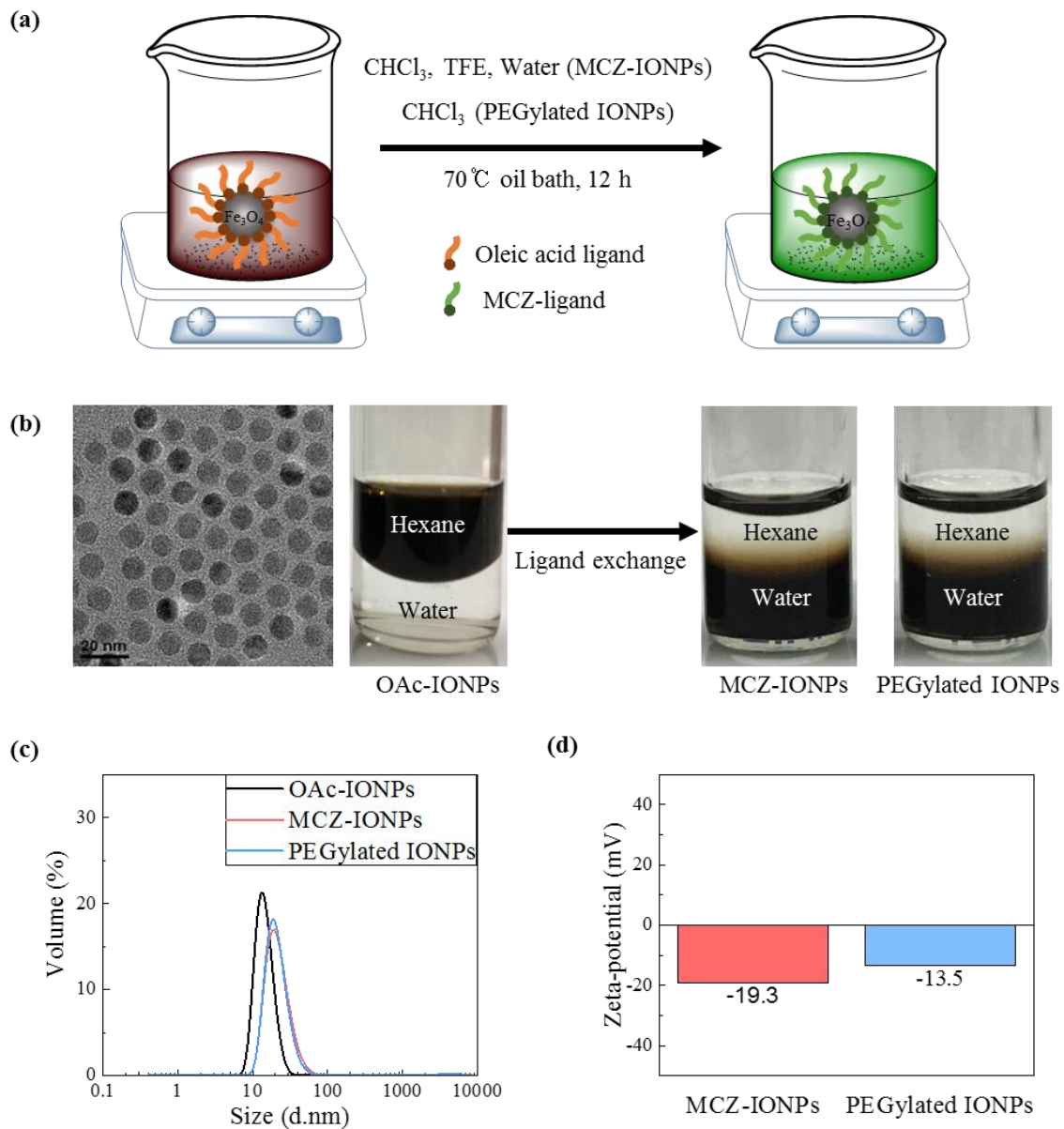
Figure 15. Surface modification of OAc-IONPs. (a) Scheme of IONPs ligand exchange. (b) TEM image of OAc-IONPs dispersed in hexane and camera images of OAc-IONPs, MCZ-IONPs, and PEGylated IONPs dispersed in hexane or water. (c) H.D and (d) zeta-potential of MCZ-IONPs and PEGylated IONPs measured by DLS.

3.3.3 Colloidal Stability and Nonspecific Binding Test

It is very important that hydrophilic IONPs should have colloidal stability in physiological condition because the unstable IONPs are likely to be agglomerated or precipitated due to interaction with biomolecule in protein rich biological media. Therefore, the colloidal stability of the MCZ-IONPs was investigated in wide pH ranges (pH 3, 5, 7, 9, 11, 13) and various concentration of saline solutions (NaCl 0.1 M, 1 M, 2 M) depending on time (1 hour, 1 day, 1 week, 1 month) by measuring H.D via DLS. The MCZ-IONPs were well dispersed in DIW, wide pH buffer solutions and various concentration saline solutions compared to PEGylated IONPs.

In the pH data, the MCZ-IONPs were well dispersed in all pH condition, from pH three to pH eleven solution for one month, without significant increase of H.D (**Figure 16a**). However, the PEGylated IONPs were aggregated after the one week in pH 3 and after one month in all the pH ranges except for pH 9. In the sodium chloride data, the MCZ-IONPs were well dispersed in various concentration of sodium chloride, while H.D of PEGylated IONPs was slightly increased in all solutions after one month (**Figure 16b**). Surprisingly, the MCZ-IONPs were stable in all conditions after one year, while the PEGylated IONPs were unstable in all pH ranges and precipitated in 2 M NaCl after 1 year (**Figure 17**). We presupposed that the zwitterion could interact with water molecules to form a hydration layer via swelling of structure, it could encapsulate the IONPs in saline solutions and prevent agglomeration even in severe conditions.[57] These results indicate that the MCZ-IONPs have excellent colloidal stability in harsh condition.

Furthermore, protein adsorption of the IONPs was investigated. In biological environment, there are various biomolecules and the biomolecules can interact with the IONPs. After the interaction, protein corona can be formed and it can directly influence colloidal stability and behavior of the IONPs in cell and in vivo. To analyze nonspecific protein adsorption of the MCZ-IONPs and PEGylated IONPs, each IONPs was incubated with BSA proteins for 30 min in 1X PBS. As a result, the both MCZ-IONPs and PEGylated IONPs were maintained the initial H.D without a size increase or aggregation after incubation with BSA **(Figure 18)**. Because the synthesized MCZ-IONPs are bipolar and negative charges induce charge repulsion, they have good dispersibility in water and superior stability in interaction with protein. Non-ionic PEG also maintained colloidal stability without adsorption because of its stealth characteristics.

(a)

(b)
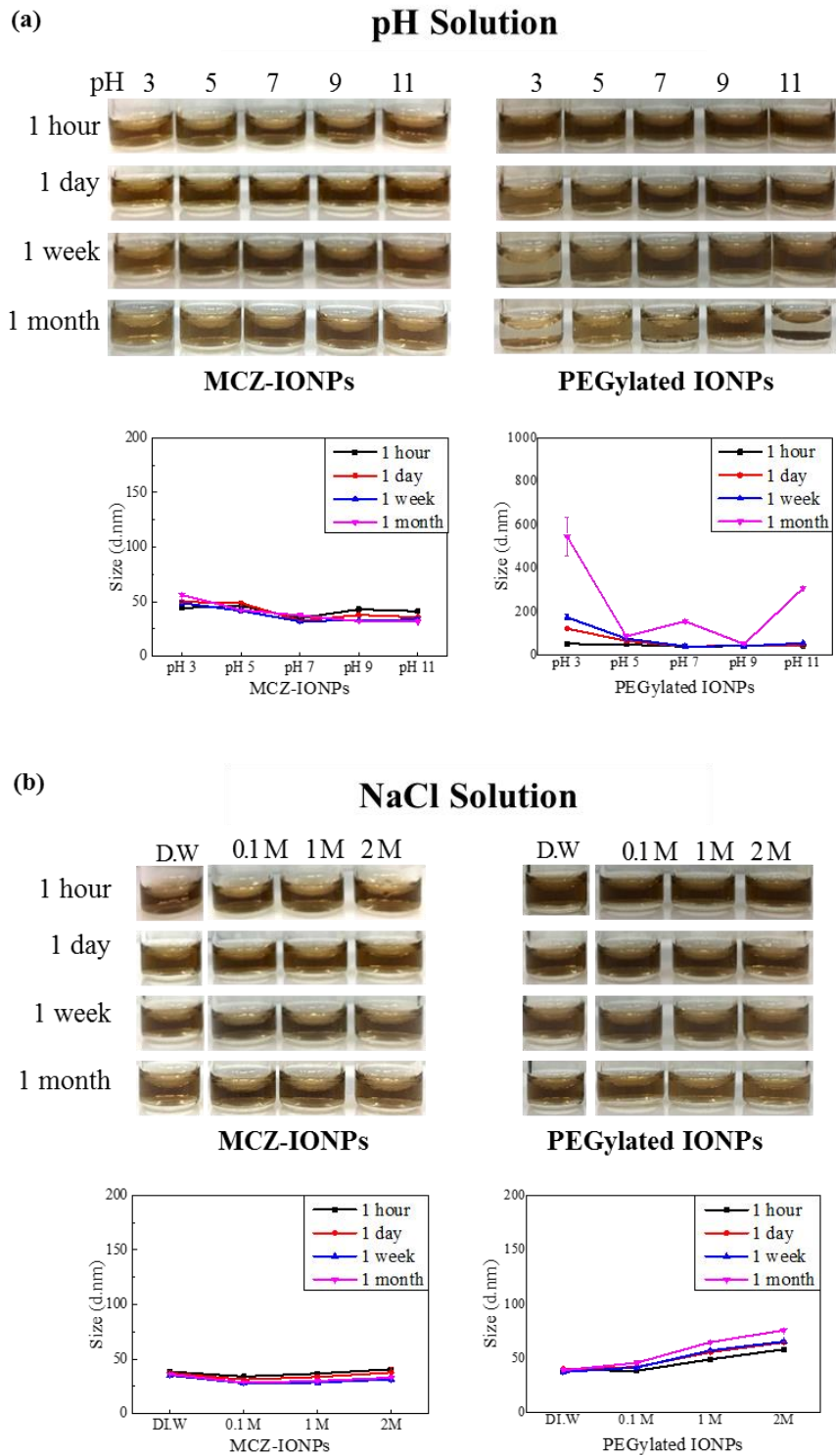
Figure 16. Stability test of MCZ-IONPs and PEGylated IONPs. (a) IONPs dispersed in wide pH buffer ranges and (b) dispersed in various concentration saline solutions for 1 month. The H.D measured by DLS.
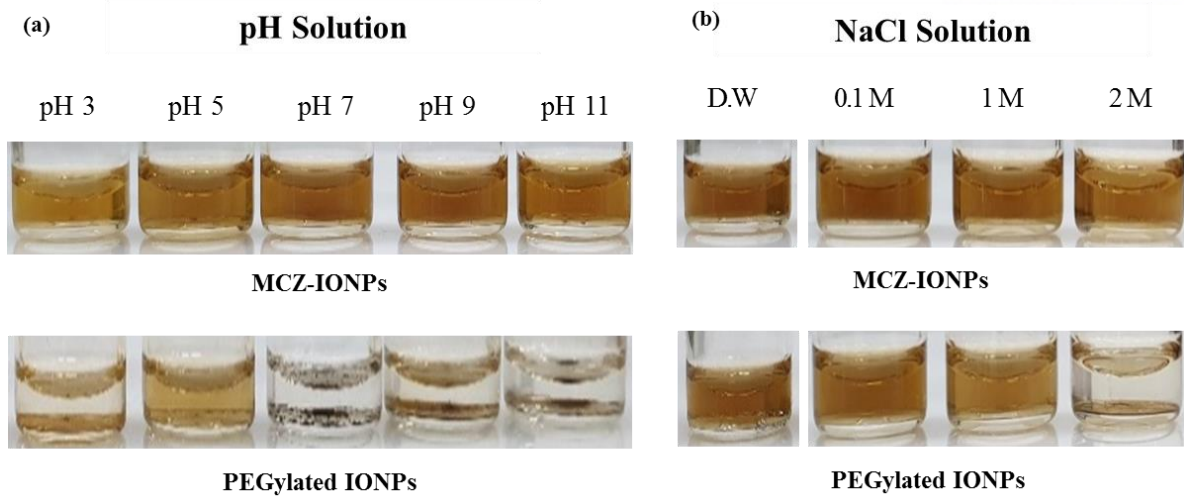
Figure 17. Stability test of MCZ-IONPs and PEGylated IONPs dispersed in wide pH buffer ranges and various concentration of saline solutions. (a) IONPs dispersed in pH buffers, and (b) dispersed in saline solutions for 1 year. The H.D measured by DLS.
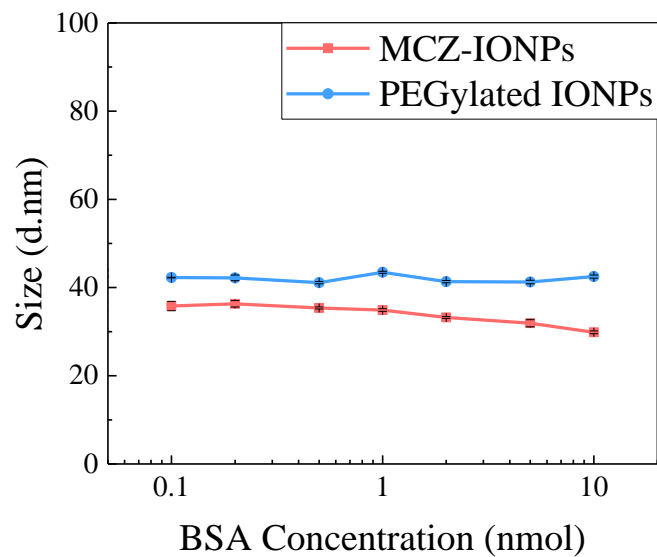
Figure 18. Nonspecific binding test of MCZ-IONPs and PEGylated IONPs with BSA proteins.

3.3.4 Bio-Functionalization

Bio-functionalization of IONPs is essential for application in various biomedical fields such as drug delivery carrier, targeting and therapeutic agent, MRI contrast agent, and imaging probe. For bio-functionalization, ligands of the IONPs need functional groups such as carboxyl group, amine group, thiol group and so on. Generally IONPs are functionalized with useful bio-molecule via carbodiimide chemistry which forms amid bond. To investigate the potential of bio-functionalization of our synthesized MCZ-IONPs, biotin and streptavidin were selected as a small molecule and large molecule respectively because biotin and streptavidin have extremely high binding affinity each other. If biotin-functionalized IONPs are mixed with a streptavidin solution at an appropriate concentration, the biotin-functionalized IONPs will be agglomerated because of the interaction between biotin and streptavidin. Conversely, if SA-IONPs are mixed with a biotin solution, the same phenomenon occurs. In this study, biotin was conjugated on surface of the MCZ-IONPs in two different methods. One is using diamine linker (**Figure 19a**). First, carboxylated zwitterionic ligand was synthesized via RAFT polymerization and the OAc-IONPs were coated with the carboxylated zwitterionic ligand. Next, the carboxylated zwitterionic IONPs were functionalized with amine groups by using diamine linker. After that, biotin was conjugated with amine group functionalized IONPs. Then, AB-IONPs were synthesized. The other method is direct functionalization biotin onto the IONPs (**Figure 19b**). First, biotinylated zwitterionic polymer was synthesized and the OAc-IONPs were coated with the biotinylated zwitterionic polymers. Then, DB-IONPs were synthesized. The former has the great advantage that we can utilize the carboxyl group or amine group of IONPs to functionalize various molecule such as drug or targeting moieties as we desired and the latter is possible of simple and reliable biotin functionalization. In the synthesis of ligand, we easily the controlled of the composition of polymers. The ratio of carboxyl group was controlled and it was analyzed by ^{1}H NMR (**Figure 20**). In NMR data, the ratio of carboxyl group was increased as more as added in polymers.

Biotinylated IONPs were aggregated in streptavidin solution because of the strong interaction (**Figure 21a**). Therefore, we confirmed interaction between biotin on the IONPs and streptavidin solution after synthesis of AB-IONPs and DB-IONPs. The H.D change of the AB-IONPs and DB-IONPs was observed after incubation with streptavidin solution, respectively. After adding the AB-IONPs to streptavidin solution, the H.D of IONPs was changed. The AB-IONPs were decreased and at the same time and the aggregated molecules were observed because of biotin-streptavidin interaction (**Figure 21b**). In case of DB-IONPs, same trend of biotin-streptavidin interaction was observed. These results indicate that both AB-IONPs and BD-IONPs were successfully functionalized with biotin molecules.

To synthesize of SA-IONPs, carbodiimide chemistry was introduced for forming amide bond between carboxyl groups of carboxylated zwitterionic IONPs and amine groups of streptavidin. The SA-IONPs were analyzed by SEM and EDX analysis. Two types silicon glass were prepared, one was treated only APTMS and the other was coated with biotin. **Figure 22a** shows scheme of interaction between SA-IONPs and silicon glass. After treatment of the SA-IONPs on each silicon glass, streptavidin-biotin interaction was observed by SEM image (**Figure 22b**). Compared to control groups coated with only APTMS, the SA-IONPs were more observed on the biotin coated silicon glass. In **Figure 22c**, an increase of iron and carbon element derived from SA-IONPs was confirmed by EDX analysis. The number and area of the SA-IONPs binding on glass were calculated as shown in **Figure 22d** and they were larger about 20 times than that of on the APTMS coated glass. These results indicate that the MCZ-IONPs were successfully functionalized with streptavidin. This means that our synthesized MCZ-IONPs have a potential of bio-functionalization with various macromolecules.

Figure 19. Synthesis of biotinylated IONPs. (a) AD-IONPs and (b) DB-IONPs.
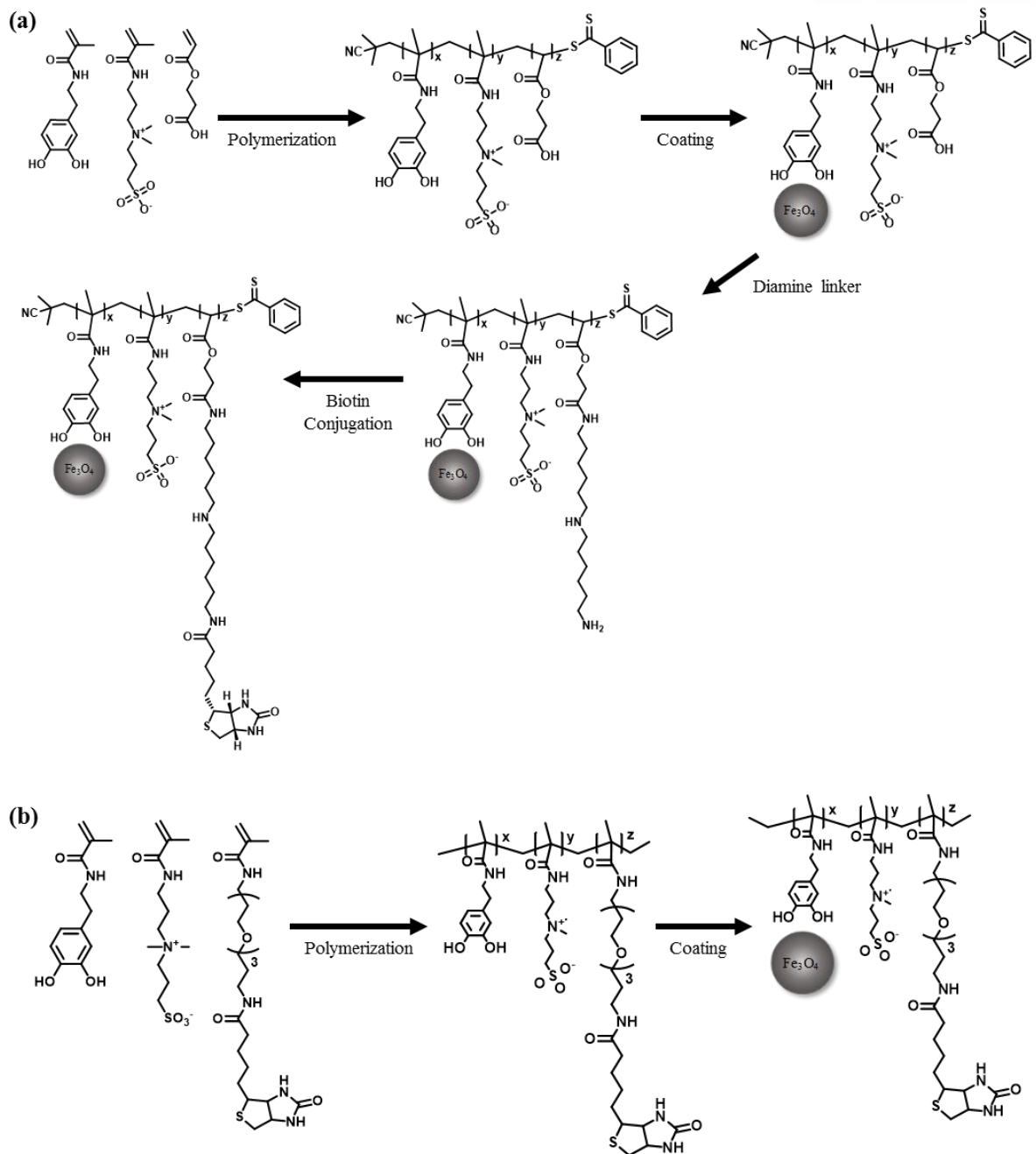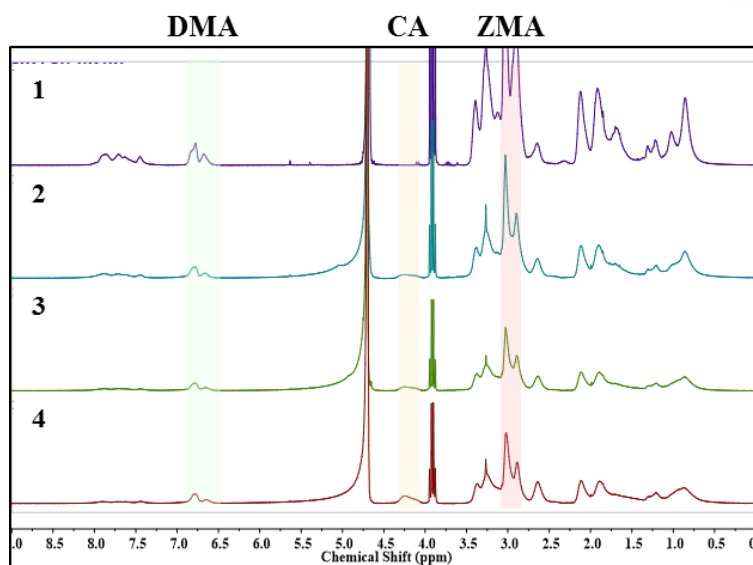
DMA : ZMA : CA		
No.	Theoretical value	Calculated value
1	20 : 80 : 0	17 : 83 : 0
2	20 : 60 : 20	18 : 68 : 14
3	20 : 50 : 30	20 : 60 : 20
4	20 : 40 : 40	19 : 52 : 29

- Dopamine methacrylamide (DMA)
- 2-carboxyethyl acrylate (CA)

Figure 20. Synthesis of carboxylated zwitterionic ligand and control of the ratio of carboxyl group in polymers. The polymer was characterized by ^{1}H NMR analysis.

(a)

(b)
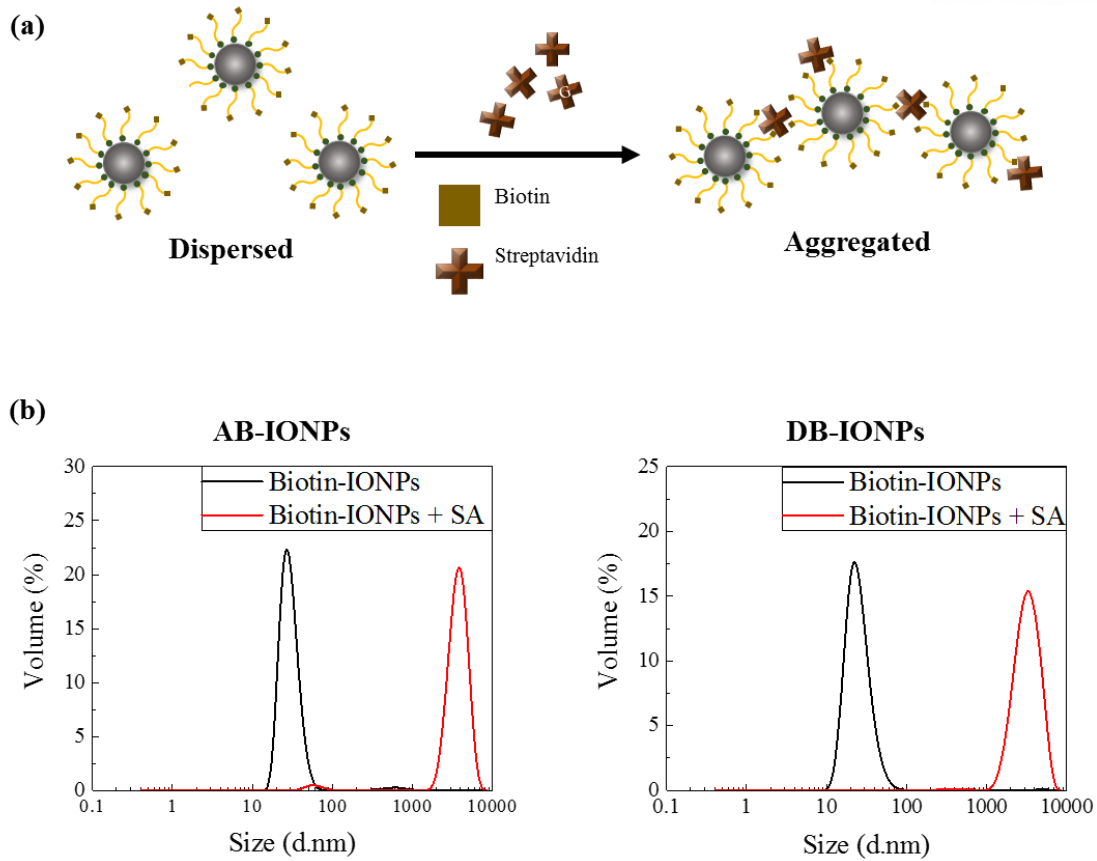
Figure 21. Biotin-streptavidin interaction. (a) Scheme of interaction between biotinylated IONPs and streptavidin in solution. (b) The H.D change of AB-IONPs and DB-IONPs after interaction with streptavidin.

(a)

(b)

Surface treated APTMS

Surface treated APTMS/Biotin

(c) Element   Atom. C [at.%]

Analysis \ Glass type	APTMS	Biotinylated APTMS
Carbon	**40.33**	**48.74**
Nitrogen	56.24	40.35
Sulfur	3.43	5.18
Iron	**0.00**	**5.73**
Total	100.00	100.00

(d)

Analysis \ Glass type	APTMS	Biotinylated APTMS
Number of IONPs (ea)	9.2	215.1
Area of IONPs (%)	2.93	68.58
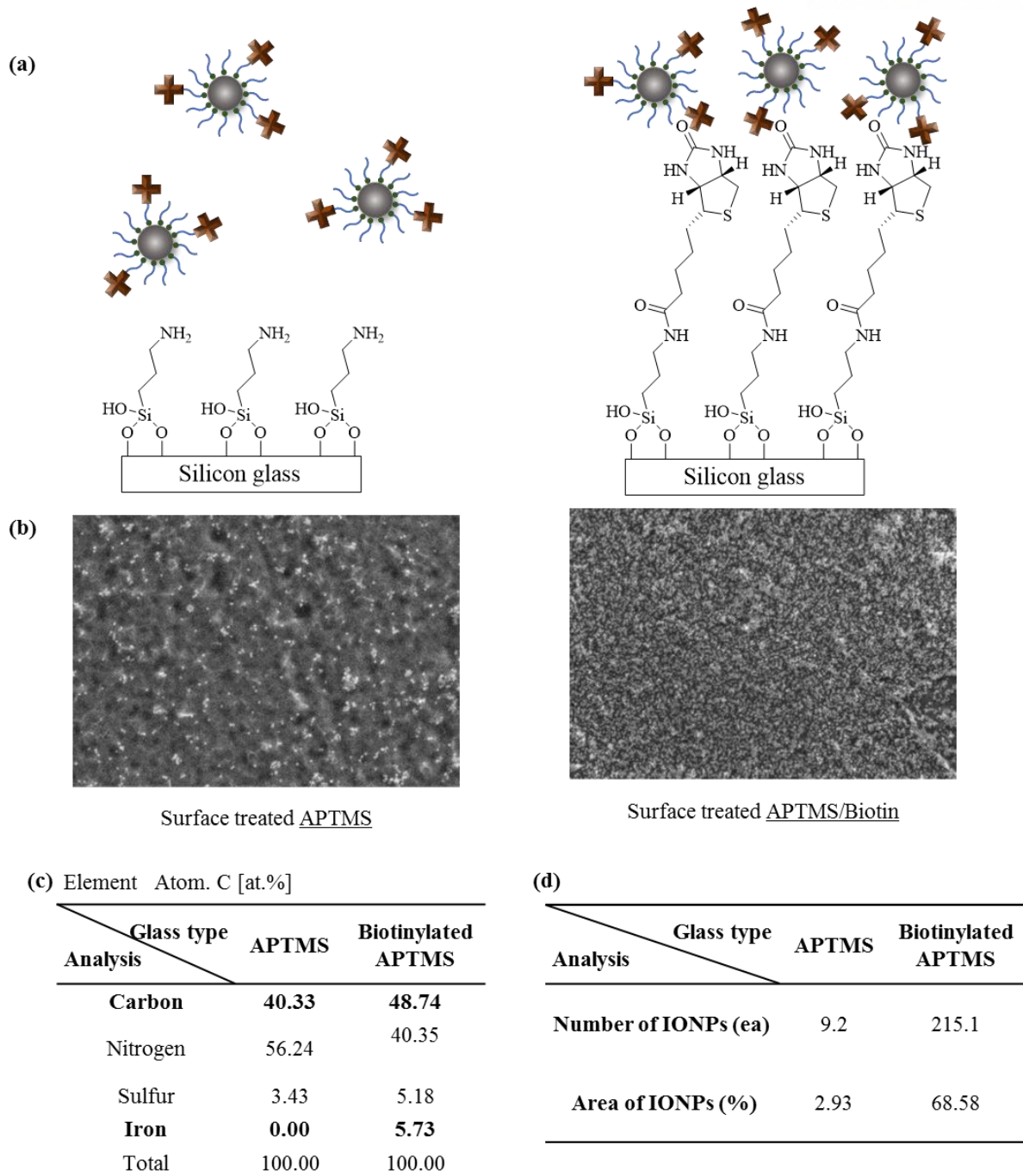
Figure 22. (a) Scheme of interaction between APTMS coated silicon glass or (b) biotin coated silicon glass and SA-IONPs. (b) SEM images, (c) EDX analysis of APTMS coated silicon glass treated SA-IONPs and biotin coated silicon glass treated SA-IONPs, and (d) summary table of IONPs number and area interaction with silicon glass.

3.4 Conclusions

In this study, we developed the MCZ-ligand by RAFT polymerization for excellent colloidal stability and easy bio-functionalization of IONPs. The MCZ-IONPs showed excellent colloidal stability at wide pH ranges and various concentrations of sodium chloride solution for 1 month and it is superior stable than PEGylated IONPs. In addition, the MCZ-IONPs showed the least nonspecific adsorption with BSA proteins. By introducing the multidentate catechol-based anchoring group, we could enhance binding affinity to IONPs. The IONPs showed good colloidal stability owing to the advantages of zwitterion. Furthermore, the MCZ-IONPs had the potential of bio-functionalization with useful bio-molecules such as biotin and streptavidin. We performed bio-functionalization of IONPs with biotin or streptavidin via strong interaction between biotin and streptavidin. We could simply synthesize functionalized ligands which have carboxyl groups, or amine groups by RAFT polymerization and conjugated streptavidin and biotin on to the IONPs. These result indicate that our MCZ-ligand provides highly excellent colloidal stability to the IONPs and this promising ligand system of IONPs can extend its ability of bio-functionalization for biomedical application.

References

(1) Mahmoudi, M.; Hofmann, H.; Rothen-Rutishauser, B.; Petri-Fink, A., Assessing the *In Vitro* and *In Vivo* Toxicity of Superparamagnetic Iron Oxide Nanoparticles. *Chem. Rev*. **2012**, *112*, 2323-2338.

(2) Hyeon, T., Chemical Synthesis of Magnetic Nanoparticles. *Chem. Commun.* **2003,** 927-934.

(3) Mahmoudi, M.; Amiri, H.; Shokrgozar, M. A.; Sasanpour, P.; Rashidian, B.; Laurent, S.; Casula, M. F.; Lascialfari, A., Raman Active Jagged-Shaped Gold-coated Magnetic Particles as a Novel Multimodal Nanoprobe. *Chem. Commun.* **2011,** *47*, 10404-10406.

(4) Zhu, N.; Ji, H. N.; Yu, P.; Niu, J. Q.; Farooq, M. U.; Akram, M. W.; Udego, I. O.; Li, H. D.; Niu, X. B., Surface Modification of Magnetic Iron Oxide Nanoparticles. *Nanomaterials* **2018,** *8,* 810-836.

(5) Bohara, R. A.; Thorat, N. D.; Pawar, S. H., Role of Functionalization: Strategies to Explore Potential Nano-Bio Applications of Magnetic Nanoparticles. *Rsc. Adv.* **2016,** *6*, 43989-44012.

(6) Ling, D. S.; Hyeon, T., Chemical Design of Biocompatible Iron Oxide Nanoparticles for Medical Applications. *Small* **2013,** *9*, 1450-1466.

(7) Patil, R. M.; Thorat, N. D.; Shete, P. B.; Otari, S. V.; Tiwale, B. M.; Pawar, S. H., *In vitro* Hyperthermia with Improved Colloidal Stability and Enhanced SAR of Magnetic Core/Shell Nanostructures. *Materials Science & Engineering C-Materials for Biological Applications* **2016,** *59*, 702-709.

(8) Chen, Y.; Yin, Q.; Ji, X. F.; Zhang, S. J.; Chen, H. R.; Zheng, Y. Y.; Sun, Y.; Qu, H. Y.; Wang, Z.; Li, Y. P.; Wang, X.; Zhang, K.; Zhang, L. L.; Shi, J. L., Manganese Oxide-Based Multifunctionalized Mesoporous Silica Nanoparticles for pH-Responsive MRI, Ultrasonography and Circumvention of MDR in Cancer Cells. *Biomaterials* **2012**, *33*, 7126-7137.

(9) Conde, J.; Dias, J. T.; Grazú, V.; Moros, M.; Baptista, P. V.; de la Fuente, J. M., Revisiting 30 years of biofunctionalization and surface chemistry of inorganic nanoparticles for nanomedicine. *Frontiers in Chemistry* **2014**, *2*, 48-74.

(10) Koniev, O.; Wagner, A., Developments and recent advancements in the field of endogenous amino acid selective bond forming reactions for bioconjugation. *Chem. Soc. Rev*. **2015**, *44*, 5495-5551.

(11) Codelli, J. A.; Baskin, J. M.; Agard, N. J.; Berozzi, C. R., Second-generation difluorinated cyclooctynes for copper-free click chemistry. *J. Am. Chem. Soc.* **2008**, *130*, 11486-11493.

(12) Ning, X. H.; Guo, J.; Wolfert, M. A.; Boons, G. J., Visualizing metabolically labeled glycoconjugates of living cells by copper-free and fast huisgen cycloadditions. *Angew. Chem. Int. Ed.*

2008, *47*, 2253-2255.

(13) Reddy, L. H.; Arias, J. L.; Nicolas, J.; Couvreur, P., Magnetic Nanoparticles: Design and Characterization, Toxicity and Biocompatibility, Pharmaceutical and Biomedical Applications. *Chem. Rev.* **2012,** *112*, 5818-5878.

(14) Markides, H.; Rotherham, M.; El Haj, A. J., Biocompatibility and Toxicity of Magnetic Nanoparticles in Regenerative Medicine. *J. Nanomater.* **2012**, *2012*, 614094-614104.

(15) Weissleder, R.; Stark, D. D.; Engelstad, B. L.; Bacon, B. R.; Compton, C. C.; White, D. L.; Jacobs, P.; Lewis, J., Superparamagnetic Iron-Oxide - Pharmacokinetics and Toxicity. *Am. J. Roentgenol.* **1989,** *152*, 167-173.

(16) Klausner, R. D.; Rouault, T. A.; Harford, J. B., Regulating the fate of mRNA: The Control of Cellular Iron Metabolism. *Cell* **1993,** *72,* 19-28.

(17) Bose, T.; Latawiec, D.; Mondal, P. P.; Mandal, S., Overview of Nano-Drugs Characteristics for Clinical Application: The Journey From the Entry to the Exit Point. *J. Nanopart. Res.* **2014,** *16,* 2527-2553.

(18) Laurent, S.; Dutz, S.; Hafeli, U. O.; Mahmoudi, M. Magnetic fluid hyperthermia: Focus on Superparamagnetic Iron Oxide Nanoparticles. *Adv. Colloid Interface Sci.* **2011**, *166*, 8-23.

(19) Xie, J.; Liu, G.; Eden, H. S.; Ai, H.; Chen, X. Y. Surface-Engineered Magnetic Nanoparticle Platforms for Cancer Imaging and Therapy. *Acc. Chem. Res.* **2011**, *44*, 883-892.

(20) Yoo, D.; Lee, J. H.; Shin, T. H.; Cheon, J. Theranostic Magnetic Nanoparticles. *Acc. Chem. Res.* **2011**, *44*, 863-874.

(21) Mahmoudi, M.; Hosseinkhani, H.; Hosseinkhani, M.; Boutry, S.; Simchi, A.; Journeay, W. S.; Subramani, K.; Laurent, S. Magnetic Resonance Imaging Tracking of Stem Cells *in Vivo* Using Iron Oxide Nanoparticles as a Tool for the Advancement of Clinical Regenerative Medicine. *Chem. Rev.* **2011**, *111*, 253-280.

(22) Colombo, M.; Carregal-Romero, S.; Casula, M. F.; Gutierrez, L.; Morales, M. P.; Bohm, I. B.; Heverhagen, J. T.; Prosperi, D.; Parak, W. J. Biological Applications of Magnetic Nanoparticles. *Chem. Soc. Rev.* **2012**, *41*, 4306-4334.

(23) Pan, Y.; Du, X. W.; Zhao, F.; Xu, B. Magnetic Nanoparticles for the Manipulation of Proteins and Cells. *Chem. Soc. Rev.* **2012**, *41*, 2912-2942.

(24) Na, H. B.; Palui, G.; Rosenberg, J. T.; Ji, X.; Grant, S. C.; Mattoussi, H. Multidentate Catechol-Based Polyethylene Glycol Oligomers Provide Enhanced Stability and Biocompatibility to Iron Oxide Nanoparticles. *ACS Nano* **2012**, *6*, 389-399.

(25) Li, P.; Chevallier, P.; Ramrup, P.; Biswas, D.; Vuckovich, D.; Fortin, M.-A.; Oh, J. K. Mussel-Inspired Multidentate Block Copolymer to Stabilize Ultrasmall Superparamagnetic Fe3O4 for Magnetic Resonance Imaging Contrast Enhancement and Excellent Colloidal Stability. *Chem. Mater.* **2015**, *27*, 7100-7109.

(26) Amstad, E.; Textor, M.; Reimhult, E. Stabilization and Functionalization of Iron Oxide Nanoparticles for Biomedical Applications. *Nanoscale* **2011**, *3*, 2819-2843.

(27) Ling, D.; Lee, N.; Hyeon, T. Chemical Synthesis and Assembly of Uniformly Sized Iron Oxide Nanoparticles for Medical Applications. *Acc. Chem. Res.* **2015**, *48*, 1276-1285.

(28) Fröhlich, E. The role of surface charge in cellular uptake and cytotoxicity of medical nanoparticles. *Int. J. Nanomed.* **2012**, *7*, 5577-5591.

(29) Hanot, C. C.; Choi, Y. S.; Anani, T. B.; Soundarrajan, D.; David, A. E. Effects of Iron-Oxide Nanoparticle Surface Chemistry on Uptake Kinetics and Cytotoxicity in CHO-K1 Cells. *Int. J. Mol. Sci.* **2016**, *17*, 54-68.

(30) Mahmoudi, M.; Laurent, S.; Shokrgozar, M. A.; Hosseinkhani, M. Toxicity Evaluations of Superparamagnetic Iron Oxide Nanoparticles: Cell "Vision" versus Physicochemical Properties of Nanoparticles. *ACS Nano* **2011**, *5*, 7263-7276.

(31) Di Bona, K. R.; Xu, Y. L.; Ramirez, P. A.; DeLaine, J.; Parker, C.; Bao, Y. P.; Rasco, J. F. Surface Charge and Dosage Dependent Potential Developmental Toxicity and Biodistribution of Iron Oxide Nanoparticles in Pregnant CD-1 mice. *Reprod. Toxicol.* **2014**, *50*, 36-42.

(32) Barrow, M.; Taylor, A.; Nieves, D. J.; Bogart, L. K.; Mandal, P.; Collins, C. M.; Moore, L. R.; Chalmers, J. J.; Lévy, R.; Williams, S. R.; Murray, P.; Rosseinsky, M. J.; Adams, D. J. Tailoring the Surface Charge of Dextran-Based Polymer Coated SPIONs for Modulated Stem Cell Uptake and MRI Contrast. *Biomater. Sci.* **2015**, *3*, 608-616.

(33) Sakulkhu, U.; Mahmoudi, M.; Maurizi, L.; Coullerez, G.; Hofmann-Amtenbrink, M.; Vries, M.; Motazacker, M.; Rezaee, F.; Hofmann, H. Significance of Surface Charge and Shell Material of Superparamagnetic Iron Oxide Nanoparticle (SPION) Based Core/Shell Nanoparticles on the Composition of the Protein Corona. *Biomater. Sci.* **2015**, *3*, 265-278.

(34) Calatayud, M. P.; Sanz, B.; Raffa, V.; Riggio, C.; Ibarra, M. R.; Goya, G. F. The effect of surface charge of functionalized Fe3O4 nanoparticles on protein adsorption and cell uptake. *Biomaterials* **2014**, *35*, 6389-6399.18.

(35) Ayala, V.; Herrera, A. P.; Latorre-Esteves, M.; Torres-Lugo, M.; Rinaldi, C. Effect of surface charge on the colloidal stability and in vitro uptake of carboxymethyl dextran-coated iron oxide nanoparticles. *J. Nanopart. Res.* **2013**, *15*, 1874-1887.

(36) Rivet, C. J.; Yuan, Y.; Borca-Tasciuc, D. A.; Gilbert, R. J. Altering Iron Oxide Nanoparticle Surface Properties Induce Cortical Neuron Cytotoxicity. *Chem. Res. Toxicol.* **2012**, *25*, 153-161

(37) Liu, W. H.; Greytak, A. B.; Lee, J.; Wong, C. R.; Park, J.; Marshall, L. F.; Jiang, W.; Curtin, P. N.; Ting, A. Y.; Nocera, D. G.; Fukumura, D.; Jain, R. K.; Bawendi, M. G. Compact Biocompatible Quantum Dots via RAFT-Mediated Synthesis of Imidazole-Based Random Copolymer Ligand. *J. Am. Chem. Soc.* **2010**, *132*, 472-483.

(38) Saito, Y.; Kawano, T.; Shimomura, M.; Yabu, H. Fabrication of Mussel-Inspired Highly Adhesive Honeycomb Films Containing Catechol Groups and Their Applications for Substrate-Independent Porous Templates. *Macromol. Rapid Commun.* **2013**, *34*, 630-634.

(39) Aoyagi, N.; Endo, T. Functional RAFT Agents for Radical-Controlled Polymerization: Quantitative Synthesis of Trithiocarbonates Containing Functional Groups as RAFT Agents Using Equivalent Amount of CS2. *J. Polym. Sci., Part A: Polym. Chem.* **2009**, *47*, 3702-3709.

(40) Park, J.; An, K. J.; Hwang, Y. S.; Park, J. G.; Noh, H. J.; Kim, J. Y.; Park, J. H.; Hwang, N. M.; Hyeon, T. Ultra-large-scale syntheses of monodisperse nanocrystals. *Nat. Mater.* **2004**, *3*, 891-895.

(41) Park, Y.; Whitaker, R. D.; Nap, R. J.; Paulsen, J. L.; Mathiyazhagan, V.; Doerrer, L. H.; Song, Y. Q.; Hurlimann, M. D.; Szleifer, I.; Wong, J. Y. Stability of Superparamagnetic Iron Oxide Nanoparticles at Different pH Values: Experimental and Theoretical Analysis. *Langmuir* **2012**, *28*, 6246-6255.

(42) Laurent, S.; Forge, D.; Port, M.; Roch, A.; Robic, C.; Elst, L. V.; Muller, R. N. Magnetic Iron Oxide Nanoparticles: Synthesis, Stabilization, Vectorization, Physicochemical Characterizations, and Biological Applications. *Chem. Rev.* **2008**, *108*, 2064-2110.

(43) Pisciotti, M. L. M.; Lima, E.; Mansilla, M. V.; Tognoli, V. E.; Troiani, H. E.; Pasa, A. A.; Creczynski-Pasa, T. B.; Silva, A. H.; Gurman, P.; Colombo, L.; Goya, G. F.; Lamagna, A.; Zysler, R. D. *In Vitro* and *In Vivo* Experiments with Iron Oxide Nanoparticles Functionalized with Dextran or Polyethylene Glycol for Medical Applications: Magnetic targeting. *J. Biomed. Mater. Res., Part B* **2014**, *102*, 860-868.

(44) Cole, A. J.; David, A. E.; Wang, J. X.; Galban, C. J.; Hill, H. L.; Yang, V. C. Polyethylene Glycol Modified, Cross-Linked Starch-Coated Iron Oxide Nanoparticles for Enhanced Magnetic Tumor Targeting. *Biomaterials* **2011**, *32*, 2183-2193.

(45) Wiogo, H. T. R.; Lim, M.; Bulmus, V.; Yun, J.; Amal, R. Stabilization of Magnetic Iron Oxide Nanoparticles in Biological Media by Fetal Bovine Serum (FBS). *Langmuir* **2011**, *27*, 843-850.

(46) Khan, M. I.; Mohammad, A.; Patil, G.; Naqvi, S. A. H.; Chauhan, L. K. S.; Ahmad, I. Induction of ROS, Mitochondrial Damage and Autophagy in Lung Epithelial Cancer Cells by Iron Oxide Nanoparticles. *Biomaterials* **2012**, *33*, 1477-1488.

(47) Patil, U. S.; Adireddy, S.; Jaiswal, A.; Mandava, S.; Lee, B. R.; Chrisey, D. B. *In Vitro/In Vivo* Toxicity Evaluation and Quantification of Iron Oxide Nanoparticles. *Int. J. Mol. Sci.* **2015**, *16*, 24417-24450.

(48) Zhang, P.; Jain, P.; Tsao, C.; Yuan, Z. F.; Li, W. C.; Li, B. W.; Wu, K.; Hung, H. C.; Lin, X. J.; Jiang, S. Y. Polypeptides with High Zwitterion Density for Safe and Effective Therapeutics. *Angew. Chem. Int. Ed.* **2018,** *57*, 7743-7747.

(49) Lee, N.; Yoo, D.; Ling, D.; Cho, M. H.; Hyeon, T.; Cheon, J., Iron Oxide Based Nanoparticles for Multimodal Imaging and Magnetoresponsive Therapy. *Chem. Rev.* **2015**, *115*, 10637-10689.

(50) Mykhaylyk, O.; Sobisch, T.; Almstatter, I.; Sanchez-Antequera, Y.; Brandt, S.; Anton, M.; Doblinger, M.; Eberbeck, D.; Settles, M.; Braren, R.; Lerche, D.; Plank, C., Silica-Iron Oxide Magnetic Nanoparticles Modified for Gene Delivery: A Search for Optimum and Quantitative Criteria. *Pharm. Res.* **2012**, *29*, 1344-1365.

(51) Blanco-Andujar, C.; Walter, A.; Cotin, G.; Bordeianu, C.; Mertz, D.; Felder-Flesch, D.; Begin-Colin, S., Design of Iron Oxide-Based Nanoparticles for MRI and Magnetic Hyperthermia. *Nanomedicine* **2016**, *11*, 1889-1910.

(52) Liu, G.; Gao, J. H.; Ai, H.; Chen, X. Y., Applications and Potential Toxicity of Magnetic Iron Oxide Nanoparticles. *Small* **2013**, *9*, 1533-1545.

(53) Palui, G.; Aldeek, F.; Wang, W.; Mattoussi, H., Strategies for interfacing inorganic nanocrystals with biological systems based on polymer-coating. *Chem. Soc. Rev.* **2015**, *44*, 193-227.

(54) Zhang, Q.; Nurumbetov, G.; Simula, A.; Zhu, C. Y.; Li, M. X.; Wilson, P.; Kempe, K.; Yang, B.; Tao, L.; Haddleton, D. M., Synthesis of Well-Defined Catechol Polymers for Surface Functionalization of Magnetic Nanoparticles. *Polym. Chem.* **2016**, *7*, 7002-7010.

(55) Wang, W. T.; Ji, X.; Na, H. B.; Safi, M.; Smith, A.; Palui, G.; Perez, J. M.; Mattoussi, H., Design of a Multi-Dopamine-Modified Polymer Ligand Optimally Suited for Interfacing Magnetic

Nanoparticles with Biological Systems. *Langmuir* **2014**, *30*, 6197-6208.

(56) Mondini, S.; Leonzino, M.; Drago, C.; Ferretti, A. M.; Usseglio, S.; Maggioni, D.; Tornese, P.; Chini, B.; Ponti, A., Zwitterion-Coated Iron Oxide Nanoparticles: Surface Chemistry and Intracellular Uptake by Hepatocarcinoma (HepG2) Cells. *Langmuir* **2015**, *31*, 7381-7390.

(57) Demillo, V. G.; Zhu, X. S., Zwitterionic Amphiphile Coated Magnetofluorescent Nanoparticles-Synthesis, Characterization and Tumor Cell Targeting. *J. Mater. Chem.* **2015**, *3*, 8328-8336.

(58) Wang, J.; Yuan, S. M.; Zhang, Y. J.; Wu, W.; Hu, Y.; Jiang, X. Q., The Effects of Poly(Zwitterions)s Versus Poly(Ethylene Glycol) Surface Coatings on the Biodistribution of Protein Nanoparticles. *Biomater. Sci.* **2016**, *4*, 1351-1360.

(59) Zhan, N. Q.; Palui, G.; Safi, M.; Ji, X.; Mattoussi, H., Multidentate Zwitterionic Ligands Provide Compact and Highly Biocompatible Quantum Dots. *J. Am. Chem. Soc.* **2013**, *135*, 13786-13795.

(60) Wang, W. T.; Ji, X.; Kapur, A.; Zhang, C. Q.; Mattoussi, H., A Multifunctional Polymer Combining the Imidazole and Zwitterion Motifs as a Biocompatible Compact Coating for Quantum Dots. *J. Am. Chem. Soc.* **2015**, *137*, 14158-14172.

(61) Aldeek, F.; Muhammed, M. A. H.; Palui, G.; Zhan, N. Q.; Mattoussi, H., Growth of Highly Fluorescent Polyethylene Glycol- and Zwitterion-Functionalized Gold Nanoclusters. *Acs Nano* **2013**, *7*, 2509-2521.

(62) Hu, R.; Li, G. Z.; Jiang, Y. J.; Zhang, Y.; Zou, J. J.; Wang, L.; Zhang, X. W., Silver-Zwitterion Organic-Inorganic Nanocomposite with Antimicrobial and Antiadhesive Capabilities. *Langmuir* **2013**, *29*, 3773-3779.

(63) Yang, W.; Zhang, L.; Wang, S. L.; White, A. D.; Jiang, S. Y., Functionalizable and Ultra Stable Nanoparticles Coated with Zwitterionic Poly(Carboxybetaine) in Undiluted Blood Serum. *Biomaterials* **2009**, *30*, 5617-5621.

(64) Yuan, J. J.; Armes, S. P.; Takabayashi, Y.; Prassides, K.; Leite, C. A. P.; Galembeck, F.; Lewis, A. L., Synthesis of Biocompatible Poly 2-(Methacryloyloxy)Ethyl Phosphorylcholine-Coated Magnetite Nanoparticles. *Langmuir* **2006**, *22*, 10989-10993.

(65) Xiao, W. C.; Lin, J.; Li, M. L.; Ma, Y. J.; Chen, Y. X.; Zhang, C. F.; Li, D.; Gu, H. C., Prolonged *In Vivo* Circulation Time by Zwitterionic Modification of Magnetite Nanoparticles for Blood Pool Contrast Agents. *Contrast Media Mol. Imaging* **2012**, *7*, 320-327.

(66) Wei, H.; Insin, N.; Lee, J.; Han, H. S.; Cordero, J. M.; Liu, W. H.; Bawendi, M. G., Compact Zwitterion-Coated Iron Oxide Nanoparticles for Biological Applications. *Nano Lett.* **2012**, *12*, 22-25.

Acknowledge (감사의 글)

2014년 2월, 기대와 열정 가득안고 연구원으로 유니스트에 첫 발을 내딛어, 어느덧 여섯번 째 여름을 보내고 있습니다. 처음 아무것도 모르고 시작하였던 대학원 생활이었던 만큼 서툴고 부족한 게 많았지만 지난 시간을 되돌아 보니 고마운 사람들이 참 많습니다. 먼저, 그 동안 연구를 배워갈 수 있는 기회를 주시고 애끓는 마음으로 지도해 주신 박종남 교수님께 감사드립니다. 졸업 논문 심사위원으로 함께해 주신 강세병 교수님, 홍성유 교수님과 연구의 길로 들어설 수 있게 방향을 잡아주신 안동대 권인숙 교수님께 감사드립니다.

MCL 여러분과 함께 지낸 시간 속에서 많이 배웠고 성숙할 수 있었습니다. 학위과정에서 뗄 수 없는 사수 현홍이, 좋을 때도 힘들 때도 함께하며 많이 도와줘서 고맙습니다. 빌게이츠 과제를 하면서 함께 고생한만큼 추억도 많이 쌓은 긍정의 아이콘 성환이와 임경이, 언제나 잘 할 수 있다고 격려해 주며 가르쳐주는 것에 넉넉했던 현중이와 용훈이, 앞으로 MCL 을 이끌어 갈 강용이와 성원이, 명예 MCL 멤버 도훈이. 덕분에 잘 마칠 수 있었고 좋은 기억 많이 들고 갑니다. 그리고 MCL 에서 함께 한 요한선배, 창훈이, 성현이, 진환이, 의탁오빠, 성호오빠, 이레, 경식이, 은별이, 태윤이, 진희, 동우 모두 고맙고, 잘 되길 진심으로 바랍니다.

안정성평가 연구소에서 보낸 1년 2개월 동안 전반적인 셀 실험 및 동물실험부터 즐겁게 연구소 생활을 할 수 있도록 챙겨주신 오정화 박사님, 김수진 선생님을 비롯하여 이은희 박사님, 양희영 박사님, 세묘쌤, 미선쌤, 재환쌤, 경낭쌤, 그리고 연구와 신앙적인 부분에서 많은 힘이 되어주신 박대의 박사님께 감사드립니다. 또, 저의 어려운 순간마다 잊지 않으시고 늘 마음으로 격려해 주신 권태혁 교수님과 초기에 힘들었던 시간을 보낼 때 마음 둘 곳이 되어 주었던 ERlab 멤버분들, 특히 현규, 병만, 현오 오빠와 현탁, 광민,

덕호, 정승이, 그리고 성영 오빠에게 감사의 말씀을 전합니다. 첫 룸메였던 소연언니와 수민언니께도 감사드립니다. 덕분에 낯선 타지에서 잘 적응하며 시작할 수 있었습니다. 세포 실험에 많은 도움을 주었던 강세병 교수님 연구실에 김한솔님과 마지막까지 코웍으로 도움주신 숙명여대 신동식 교수님 연구실에 김성수님께도 감사드립니다.

무엇보다 고비의 순간마다 기도로, 맛있는 음식으로, 따뜻한 나눔과 위로의 손길로 큰 힘이 되어주신 김진욱 목자님, 조임현 목자님, 염혜림 목녀님, 박성헌 목자님, 손화정 목녀님을 비롯한 목장 식구들 지혜언니, 나경언니, 희정이, 세영이, 정우씨, 지윤이, 상우 형부, 경희 언니, 미선쌤, 정빈언니께 감사드립니다. 정말 여러분 덕분에 지금의 순간을 맞이할 수 있었습니다. 그리고, 사랑하는 친구들! 여진이, 예진이, 수진이, 한나, 선희, 희영이, 예원이, 미선이, 아영이... 다들 너무 고마워. 앞으로 자주 보자!

마지막으로, 안동을 떠나 처음 울산으로 내려올 때에 아쉬운 마음 뒤로 하고 응원하며 보내주셨던 가족들, 저의 선택을 지지해 주시고 수고했다는 격려의 말로 안아주신 부모님과 진영언니, 남훈이에게도 감사의 말씀드립니다. 6년이라는 시간동안 학위 수여 뿐만 아니라, 사랑하는 사람과 가정을 이루고 새로운 가족들도 생기는 많은 변화가 있었습니다. 그 동안 많이 배려해 주시고 이해해주신 시부모님과 시댁 식구 분들, 그리고 사랑하는 남편 김정수님에게 진심으로 고맙다는 말을 전합니다. 이 모든 시간을 함께 지나온 당신이 없었다면 지금의 순간이 빛나지 못했을 것입니다. 좋은 선배이자, 동료이자, 동반자로 마지막까지 열심히 이끌줘서 고맙습니다.

그리고, 시작부터 끝까지 함께 해주신 하나님께 감사드립니다. 삶의 모든 순간 당신을 빼 놓는다면 아무 의미가 없음을 고백합니다. 새롭게 시작되는 삶에서 당신과, 그리고 모든 감사한 분들과 함께 웃음 짓는 삶을 그리며 글을 마칩니다. 모두 감사합니다.

2019. 07.

우선영 올림